

On the renormalization of Coulomb interactions in two-dimensional tilted Dirac fermions

Yu-Wen Lee*

Department of Applied Physics, Tunghai University, Taichung, Taiwan, R.O.C.

Yu-Li Lee†

Department of Physics, National Changhua University of Education, Changhua, Taiwan, R.O.C.

(Dated: March 5, 2022)

We investigate the effects of long-ranged Coulomb interactions in a tilted Dirac semimetal in two dimensions by using the perturbative renormalization-group method. Depending on the magnitude of the tilting parameter, the undoped system can have either Fermi points (type-I) or Fermi lines (type-II). Previous studies usually performed the renormalization-group transformations by integrating out the modes with large momenta. This is problematic when the Fermi surface is open, like type-II Dirac fermions. In this work, we study the effects of Coulomb interactions, following the spirit of Shankar¹, by introducing a cutoff in the energy scale around the Fermi surface and integrating out the high-energy modes. For type-I Dirac fermions, our result is consistent with that of the previous work. On the other hand, we find that for type-II Dirac fermions, the magnitude of the tilting parameter increases monotonically with lowering energies. This implies the stability of type-II Dirac fermions in the presence of Coulomb interactions, in contrast with previous results. Furthermore, for type-II Dirac fermions, the velocities in different directions acquire different renormalization even if they have the same bare values. By taking into account the renormalization of the tilting parameter and the velocities due to the Coulomb interactions, we show that while the presence of a charged impurity leads only to charge redistribution around the impurity for type-I Dirac fermions, for type-II Dirac fermions, the impurity charge is completely screened, albeit with a very long screening length. The latter indicates that the temperature dependence of physical observables are essentially determined by the RG equations we derived. We illustrate this by calculating the temperature dependence of the compressibility and specific heat of the interacting tilted Dirac fermions.

I. INTRODUCTION

The Weyl fermions in solid state materials have attracted intense theoretical and experimental interests in condensed matter community in recent years. These materials are topological since the Weyl nodes, at which the conduction and the valence bands touch in the momentum space, act as the magnetic monopoles in the momentum space². Therefore, these Weyl nodes can be characterized by the “magnetic charges” they carry. On the other hand, many of the electromagnetic responses or the transport properties of the Weyl semimetal are deeply rooted in nontrivial phenomena in the quantum field theory, such as the chiral anomaly^{3–7}. Very recently, Weyl fermions have been detected experimentally in the non-centrosymmetric but time-reversal preserving materials such as TaAs, NbAs, TaP, and NbP^{8–14}.

Due to the lack of a fundamental Lorentz symmetry, the spectra of Dirac/Weyl semimetals realized in solid state materials do not have to be isotropic. In particular, they can be tilted¹⁵. When the tilting angle is large enough, the electron and hole Fermi surfaces can coexist with the band-touching Dirac/Weyl nodes. This leads to a new kind of materials, which are commonly referred to as type-II Dirac/Weyl semimetals¹⁵. In three dimensions (3D), the tilted Weyl cones were proposed to be realized in a material WTe₂¹⁵, while in two dimensions (2D), the tilted Dirac cones were proposed to be real-

ized in a mechanically deformed graphene and the organic compound α -(BEDT-TTF)₂I₃¹⁶. Recently, type-II Dirac fermions are experimentally discovered in two materials: PdTe₂^{17,18} and PtTe₂¹⁹.

In contrast with type-I Dirac/Weyl semimetals whose Fermi surface is point-like, type-II Dirac/Weyl semimetals have an extended Fermi surface. In 2D, it consists of two straight lines crossing at the Dirac node, while it is hyperboloids touched at the Weyl nodes in 3D. Due to the nonvanishing density of states (DOS) at the Fermi energy, the physical properties of type-II Dirac/Weyl semimetals are expected to be distinct from those of type-I Dirac/Weyl semimetals. On the other hand, the open Fermi surface in the type-II materials will result in behaviors different from the usual Fermi liquid (FL) which has a closed Fermi surface. Even for type-I materials, the nonzero tilting parameter may lead to observable effects. Some theoretical studies along these directions mainly for non-interacting fermions have been performed, including the conductance and noise for tilted Dirac (2D) or Weyl fermions (3D)²⁰, longitudinal magnetoconductivity for tilted Dirac fermions²¹, thermodynamic and optical responses for tilted Weyl fermions in the presence of magnetic fields^{22–25}, anomalous Hall effect for tilted Weyl fermions^{26,27}, and anomalous Nernst and thermal Hall effect for tilted Weyl fermions^{28,29}.

In the present work, we study the effects of long-range Coulomb interactions on the tilted Dirac fermions in terms of the renormalization group (RG). Due to the van-

ishing DOS at the Fermi level, it is well-known that the Coulomb interaction for untilted Dirac fermions in 2D is marginally irrelevant in the sense of RG^{30–32}. Moreover, the value of Fermi velocity will increase at low energies. This leads to logarithmic corrections to various thermodynamic response functions, which can be computed in terms of the RG equations. The results fit the experimental data for graphene quite well³³.

What will happen for Dirac fermions in 2D when the tilting parameter is not zero? Previous RG analysis^{34,36} shows that the values of velocities also increase logarithmically toward infinity, as what happens in graphene. By taking into account the fluctuations of transverse gauge fields, the velocities of fermions are renormalized up to the speed of light at low energies³⁵. Moreover, according to the analysis in Refs. 35 and 36, the magnitude of the tilting parameter flows to zero at low energies for both types of Dirac fermions. For type-II Dirac fermions, this indicates its instability in the presence of Coulomb interactions. Within such a scenario, interacting type-II Dirac fermions is stable only when the screening length is short enough so that the above RG flow stops and turns its direction before the instability occurs.

All the above mentioned RG studies on tilted Dirac fermions employ some types of cutoff functions in the momenta, such as a direct momentum cutoff or the dimensional regularization. This is certainly fine for type-I Dirac fermions since the Fermi surface is a point. However, for systems with open Fermi surface like type-II Dirac fermions, any momentum cutoff function, which is a curve in the momentum space, will intersect with the Fermi surface. By integrating out the modes with momenta larger than the momentum cutoff to implement the RG transformation, one integrates out not only the high-energy modes but also the low-energy modes around the Fermi surface. Hence, the RG transformation is not to scale to the Fermi surface, and the conclusions about type-II Dirac fermions inferring from such a RG analysis is dubious.

As emphasized by Shankar¹, the proper way of doing RG for FL should be to scale toward the Fermi surface. The usual FL has a closed Fermi surface. Therefore, there exists a characteristic momentum, the Fermi momentum, to separate the high-energy modes from the low-energy modes. For type-II Dirac fermions, its Fermi surface is open so that such a characteristic momentum simply does not exist. To implement the RG transformation properly, we label the excitations directly by their energies and other "angle" variables. By integrating out the high-energy modes, we obtain the RG functions for velocities of fermions and the tilting parameter. Our main findings are as follows.

(i) For type-I Dirac fermions, our results are identical to the previous ones. That is, the values of velocities and the magnitude of the tilting parameter monotonically increase and decrease at low energies, respectively. This is not surprising since the Fermi surface is point-like in this case.

(ii) For type-II Dirac fermions, the values of velocities are also increase monotonically at low energies. In contrast with the previous studies, the RG functions for the two velocities of fermions are different so that they have different RG flow even if the bare values are the same. Moreover, the magnitude of the tilting parameter increases as lowering the energy, indicating the stability of type-II Dirac fermions. In other words, the long-range Coulomb interaction helps to stabilize type-II Dirac fermions, in contrast with previous studies.

(iii) In terms of the RG equations, we calculate various thermodynamic response functions for both types of Dirac fermions: the temperature dependence of specific heat at low temperatures, and the density and temperature dependence of the isothermal compressibility.

(iv) Since there is a nonzero DOS at the Fermi level for type-II Dirac fermions, it is argued that the Coulomb interaction will be screened at long distances.^{35,36} In order to address this issue, we calculate the vacuum polarization at zero frequency. We find that the polarization function is singular at zero momentum for both types of Dirac fermions. This singularity can be removed if we sum the diagrams with leading divergences in terms of RG, following the method employed in Ref. 37. From this RG-improved polarization function, we find that there is indeed complete screening for type-II Dirac fermions, albeit with a very long screening length. This indicates that the scaling of physical observables with temperatures in a large temperature range is indeed described by the RG equations we derived in this paper.

The organization of the rest of the paper is as follows. The model is defined and discussed in Sec. II. We present the RG equations and its implications in Sec. III. The calculations of thermodynamic response functions for both types of Dirac fermions are shown in Sec. IV. Sec. V is about the screening of the Coulomb potential and the Coulomb impurity problem. The last section is devoted to conclusive discussions. The details of calculations of the RG equations and the vacuum polarization are put in appendix A and B, respectively.

II. THE MODEL

We start with the minimal model of non-interacting tilted Dirac fermions described by the Hamiltonian¹⁶

$$H_0 = \sum_{\xi, \sigma, \mathbf{p}} \tilde{\psi}_{\xi\sigma}^\dagger(\mathbf{p}) (\xi w v_1 p_1 + \xi v_1 p_1 \sigma_1 + v_2 p_2) \tilde{\psi}_{\xi\sigma}(\mathbf{p}), \quad (1)$$

where $\xi = \pm 1$ denote the valley degeneracy, $\sigma = \pm 1$ account for the spin degeneracy, and $\sigma_{1,2,3}$ are the standard Pauli matrices. The fields $\tilde{\psi}_{\xi\sigma}(\mathbf{p})$ and $\tilde{\psi}_{\xi\sigma}^\dagger(\mathbf{p})$, which obey the canonical anticommutation relations, describe Dirac fermions around the Dirac nodes at the points \mathbf{K} and $-\mathbf{K}$ in the first Brillouin zone (BZ). v_1 and v_2 are the "speeds" of Dirac fermions along the x and y directions, respectively. Without loss of generality, we take

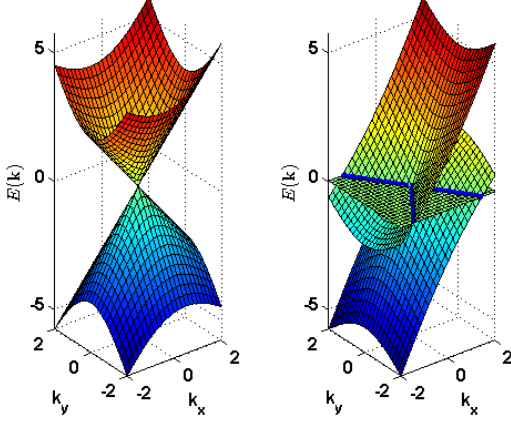


FIG. 1: Conical band structure ($\xi = 1$) for type-I Dirac fermions (left) and type-II Dirac fermions (right). For type-II Dirac fermions, the blue lines on the $E = 0$ plane indicate the Fermi surface.

$v_1, v_2 > 0$. In Eq. (1), we have set the energy of the Dirac nodes to be zero. The dimensionless constant w is the tilting parameter.

The spectrum of H_0 is given by

$$\epsilon_{\pm}(\mathbf{p}) = \xi w \tilde{p}_1 \pm \sqrt{\tilde{p}_1^2 + \tilde{p}_2^2}, \quad (2)$$

where $\tilde{p}_i = v_i p_i$ with $i = 1, 2$. It is clear that the Dirac cones are tilted along the x -axis when $w \neq 0$, as shown in Fig. 1. When $|w| < 1$, the Dirac cones are slightly tilted, corresponding to type-I Dirac fermions, while the Dirac cones are tipped over when $|w| > 1$, corresponding to type-II Dirac fermions. $|w| = 1$ are the Lifshitz transition points which separate the two types of Dirac fermions. When the chemical potential $\mu = 0$, the Fermi surface consists of two straight lines:

$$\tilde{p}_2 = \pm \tilde{w} \tilde{p}_1, \quad (3)$$

for type-II Dirac fermions, where $\tilde{w} = \sqrt{w^2 - 1}$.

The Coulomb interaction between electrons is described by the Hamiltonian

$$H_C = \frac{1}{2} \int d^2x d^2y \rho(\mathbf{x}) V(|\mathbf{x} - \mathbf{y}|) \rho(\mathbf{y}), \quad (4)$$

where $\rho(\mathbf{r}) = \sum_{\sigma=\pm} : c_{\alpha}^{\dagger}(\mathbf{r}) c_{\sigma}(\mathbf{r}) :$ is the normal-ordered electron density operator with the annihilation operator c_{σ} and creation operator c_{σ}^{\dagger} for electrons with spin- σ , and

$$V_0(\mathbf{r}) = \frac{e^2}{4\pi\epsilon r}, \quad (5)$$

is the Coulomb potential. In Eq. (5), ϵ is the dielectric constant and $-e$ is the charge carried by the electron. In terms of the low-energy degrees of freedom around the

Dirac nodes, the electron operator c_{σ} can be written as

$$c_{\sigma}(\mathbf{r}) = \sum_{\xi=\pm 1} e^{i\xi \mathbf{K} \cdot \mathbf{r}} \psi_{\xi\sigma}(\mathbf{r}) + \dots, \quad (6)$$

where the fermion field $\psi_{\xi\sigma}(\mathbf{r}) = \frac{1}{\sqrt{A}} \sum_{\mathbf{p}} e^{i\mathbf{p} \cdot \mathbf{r}} \tilde{\psi}_{\xi\sigma}(\mathbf{p})$ and A is the area of the system. With the help of Eq. (6), the density operator can be written as

$$\rho(\mathbf{r}) = \rho_0(\mathbf{r}) + [e^{-2i\mathbf{K} \cdot \mathbf{r}} M(\mathbf{r}) + \text{H.c.}] + \dots, \quad (7)$$

where $\rho_0(\mathbf{r}) = \sum_{\xi,\sigma} : \psi_{\xi\sigma}^{\dagger} \psi_{\xi\sigma}(\mathbf{r}) :$ describes the uniform component of ρ , while $M(\mathbf{r}) = \sum_{\sigma} \psi_{+\sigma}^{\dagger} \psi_{-\sigma}(\mathbf{r})$ is the order parameter for the charge-density-wave (CDW) ordering. Substituting Eq. (7) into H_c [Eq. (4)], we find that $H_c = H_{int} + \dots$, where

$$H_{int} = \frac{1}{2} \int d^2x d^2y \rho_0(\mathbf{x}) V_0(|\mathbf{x} - \mathbf{y}|) \rho_0(\mathbf{y}), \quad (8)$$

and \dots contains those terms with the factors $e^{\pm 2i\mathbf{K} \cdot \mathbf{r}}$ or $e^{\pm 2i\mathbf{K} \cdot (\mathbf{x} \pm \mathbf{y})}$. Due to the fast oscillating nature, these terms will generate short-ranged repulsive four-fermion interactions at low energies, and we shall neglect them.

Our working Hamiltonian is $H_0 + H_{int}$. When $\mu = 0$, H is invariant against the “particle-hole” (PH) transformation

$$\tilde{\psi}_{\xi\sigma}(\mathbf{p}) \rightarrow \sigma_1 \tilde{\psi}_{\xi\sigma}^*(-\mathbf{p}). \quad (9)$$

This PH symmetry forbids terms like $\tilde{\psi}_{\xi\sigma}^{\dagger} \tilde{\psi}_{\xi\sigma}$, $\tilde{\psi}_{\xi\sigma}^{\dagger} \sigma_1 \tilde{\psi}_{\xi\sigma}$, or $\tilde{\psi}_{\xi\sigma}^{\dagger} \sigma_2 \tilde{\psi}_{\xi\sigma}$ since they are odd under the PH transformation. We shall see later that this PH symmetry together with gauge invariance guarantee the renormalizability of this theory.

III. THE RG EQUATIONS

To derive the RG equation, we perform a Hubbard-Stratonovich transformation so that the action in the imaginary-time formulation can be written as

$$S = \sum_{\xi,\alpha} \int_X \psi_{\xi\alpha}^{\dagger} [\partial_{\tau} - i\xi v_1 (w + \sigma_1) \partial_1 - i v_2 \sigma_2 \partial_2] \psi_{\xi\alpha} + \int_Q \frac{|\mathbf{q}|}{g^2} \tilde{\phi}^{\dagger}(Q) \tilde{\phi}(Q) + i \int_X \phi(X) \rho_0(X), \quad (10)$$

where $Q = (iq_0, \mathbf{q})$, $X = (\tau, \mathbf{x})$, $g^2 = e^2/\epsilon$, $\int_X = \int d\tau d^2x$, $\int_Q = \int \frac{dq_0}{2\pi} \frac{d^2q}{(2\pi)^2}$, and $\tilde{A}(Q)$ denotes the Fourier transform of $A(X)$. Since the auxiliary field $\phi(X)$ is real, $\tilde{\phi}^{\dagger}(Q) = \tilde{\phi}(-Q)$. We have extended the number of fermion fields to N pairs such that $\alpha = 1, 2, \dots, N$. Physically, $N = 2$ due to the spin degeneracy. S still preserves the PH symmetry as long as we require that ϕ transforms as

$$\phi \rightarrow -\phi, \quad (11)$$

under the PH transformation.

As we have discussed in the introduction, the proper way to implement the RG transformation for a system with an open Fermi surface is to integrate out an energy shell each time, instead of a momentum shell. To achieve this goal, we have to parametrize the equal-energy curves first. These curves are given by the equations $\epsilon_{\pm}(\mathbf{p}) = E$. For type-I Dirac fermions ($|w| < 1$), these equal-energy curves are ellipses and can be parametrized as

$$\begin{aligned}\tilde{p}_1 &= -\frac{\xi w}{1-w^2}E + \frac{|E|}{1-w^2}\cos\theta, \\ \tilde{p}_2 &= \frac{|E|}{\sqrt{1-w^2}}\sin\theta,\end{aligned}\quad (12)$$

for given E , where $0 \leq \theta < 2\pi$. On the other hand, for type-II Dirac fermions ($|w| > 1$), these equal-energy curves are hyperbolas and can be parametrized as

$$\begin{aligned}\tilde{p}_1 &= \frac{\xi w}{w^2-1}E \pm \frac{|E|}{w^2-1}\cosh\theta, \\ \tilde{p}_2 &= \frac{|E|}{\sqrt{w^2-1}}\sinh\theta,\end{aligned}\quad (13)$$

for given E , where $-\infty < \theta < +\infty$. In Eq. (13), the $+$ and $-$ signs correspond to the right and the left branches of the hyperbola, respectively.

In terms of the parametrization (12) or (13), the momentum integral can be written as

$$\int d^2\tilde{p} = \frac{1}{2} \int_{-\Lambda}^{\Lambda} \frac{|E|dE}{(1-w^2)^{3/2}} \int_0^{2\pi} d\theta (1 - \eta_E \xi w \cos\theta), \quad (14)$$

for type-I Dirac fermions, and

$$\begin{aligned}\int d^2\tilde{p} &= \frac{1}{2} \int_{-\Lambda}^{\Lambda} \frac{|E|dE}{\tilde{w}^3} \left[\int_{-\infty}^{+\infty} d\theta (|w| \cosh\theta + \eta_E \eta_w \xi) \right. \\ &\quad \left. + \int_{-\infty}^{+\infty} d\theta (|w| \cosh\theta - \eta_E \eta_w \xi) \right],\end{aligned}\quad (15)$$

for type-II Dirac fermions, where Λ is the UV cutoff in energies and $\eta_A = \text{sgn}A$. In Eq. (15), the first and the second θ integrals for given E correspond to the integrations over the right and the left branches of the hyperbola, respectively. In fact, it suffices to consider the integrals over $E > 0$ or $E < 0$ since the involved two bands have been taken into account by the Pauli matrices. However, this regularization breaks the PH symmetry at $\mu = 0$. Hence, we define the momentum integral by Eqs. (14) or (15), and include a prefactor $1/2$.

Before plunging into the calculation of the RG equations, we discuss some constraints on the renormalization of the various terms in the action S . First of all, S is invariant against the gauge transformation:

$$\psi_{\xi\alpha} \rightarrow e^{-i\chi(\tau)}\psi_{\xi\alpha}, \quad \phi \rightarrow \phi + \partial_{\tau}\chi. \quad (16)$$

By integrating out the fast modes which have energies within the range $(\Lambda/s, \Lambda)$ with $s = e^l > 1$, S becomes

$$\begin{aligned}S \rightarrow & (1 + \Sigma_{\tau}) \sum_{\xi,\alpha} \int_X \psi_{\xi\alpha}^{\dagger} \partial_{\tau} \psi_{\xi\alpha} + (1 + \Gamma_0) i \int_X \phi \rho_0 \\ & + \sum_{\xi,\alpha} \int_X \psi_{\xi\alpha}^{\dagger} \mathcal{H}_0 \psi_{\xi\alpha} + \int_Q \frac{|\mathbf{q}|}{g^2} \tilde{\phi}^{\dagger}(Q) \tilde{\phi}(Q) + \dots,\end{aligned}$$

where \dots denotes the terms with higher scaling dimensions. Here we do not explicitly write down the renormalized Hamiltonian \mathcal{H}_0 since it is irrelevant in the derivation of the Ward identity. The gauge invariance leads to the Ward identity^{30,38}

$$\Sigma_{\tau} = \Gamma_0. \quad (17)$$

Next, the non-analytic dependence of the $|\mathbf{q}|/g^2$ term on \mathbf{q} prohibits its renormalization under integrating out the fast modes^{30,38}. Thus, it is not necessary to introduce the wavefunction renormalization of the ϕ field. This fact together with Eq. (17) result in the non-renormalization of g^2 .

We now integrate out the fast modes to the one-loop order to get the RG equations by assuming the weak-coupling limit $g^2/\sqrt{v_1 v_2} \ll 1$. From the above discussions, it suffices to compute the self-energy of fermions. After integrating out the fast modes and rescaling the energy, angle variable, frequency, and fields by $E \rightarrow s^{-1}E$, $\theta \rightarrow \theta$, $p_0 \rightarrow s^{-1}p_0$, $\tilde{\psi}_{\xi\alpha} \rightarrow s^2 Z_{\psi}^{-1/2} \tilde{\psi}_{\xi\alpha}$, and $\tilde{\phi} \rightarrow s^2 \tilde{\phi}$, we find the following facts: (i) $\Sigma_{\tau} = O(g^4/v_1 v_2)$ to the one-loop order, which leads to $Z_{\psi} = 1 + O(g^4/v_1 v_2)$ for both types of Dirac fermions. (ii) v_1 and v_2 acquire nontrivial renormalization. (iii) $w v_1$ is not renormalized to the one-loop order for type-I Dirac fermions, while it acquires nontrivial renormalization for type-II Dirac fermions. The details of the calculations are left to appendix A.

The resulting one-loop RG equations for type-I Dirac fermions are

$$\frac{dv_l}{dl} = \frac{g^2}{16\pi}, \quad \frac{d}{dl}(w_l v_l) = 0, \quad (18)$$

where the quantities with the subscript l indicate the renormalized parameters, while those without the subscript l correspond to the bare ones. Here we have taken $v_1 = v_2 = v$. Equation (18) is identical to the one in Ref. 34. On the other hand, the one-loop RG equations for type-II Dirac fermions are

$$\frac{dv_{1l}}{dl} = \frac{\tilde{w}_l g^2 r_l}{8\pi^2} M_1(|w_l|, r_l), \quad (19)$$

$$\frac{dv_{2l}}{dl} = \frac{\tilde{w}_l^3 g^2 r_l^2}{8\pi^2} M_2(|w_l|, r_l), \quad (20)$$

and

$$\frac{d|w_l|}{dl} = \frac{\tilde{w}_l g^2 r_l}{8\pi^2 v_{1l}} \mathcal{N}(|w_l|, r_l), \quad (21)$$

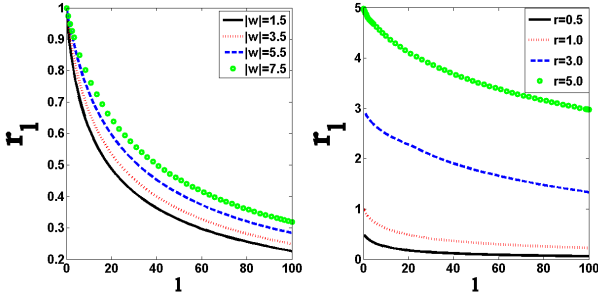


FIG. 2: The RG flow of the ratio $r_l = v_{1l}/v_{2l}$ with $r(0) = 1$ and various values of $|w|$ (left) and with $|w| = 1.5$ and various values of r (right) for type-II Dirac fermions. In both diagrams, we have taken $v_2 = 1.3g^2/(4\pi)$.

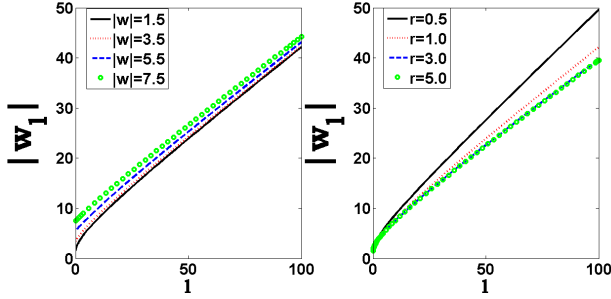


FIG. 3: The RG flow of $|w_l|$ with $r = 1$ and various values of $|w|$ (left) and with $|w| = 1.5$ and various values of r (right) for type-II Dirac fermions. In both diagrams, we have taken $v_2 = 1.3g^2/(4\pi)$.

where $r_l = v_{1l}/v_{2l}$,

$$M_1 = \int_{\ln|w|}^{+\infty} d\theta \frac{(|w| - \cosh \theta)^2}{[(|w| - \cosh \theta)^2 + r^2 \tilde{w}^2 \sinh^2 \theta]^{3/2}},$$

$$M_2 = \int_{\ln|w|}^{+\infty} d\theta \frac{\sinh^2 \theta}{[(|w| - \cosh \theta)^2 + r^2 \tilde{w}^2 \sinh^2 \theta]^{3/2}},$$

and

$$\mathcal{N} = \int_0^{+\infty} d\theta \frac{(|w| \cosh \theta + 1)(|w| + \cosh \theta)}{[(|w| + \cosh \theta)^2 + r^2 \tilde{w}^2 \sinh^2 \theta]^{3/2}} \\ + \int_0^{+\infty} d\theta \frac{(|w| \cosh \theta - 1)(|w| - \cosh \theta)}{[(|w| - \cosh \theta)^2 + r^2 \tilde{w}^2 \sinh^2 \theta]^{3/2}} \\ - \int_{\ln|w|}^{+\infty} d\theta \frac{\tilde{w}^2 (|w| - \cosh \theta)}{[(|w| - \cosh \theta)^2 + r^2 \tilde{w}^2 \sinh^2 \theta]^{3/2}}.$$

Since $M_1, M_2, r > 0$, Eqs. (19) and (20) indicate that the values of v_{1l} and v_{2l} become large at low energies. This implies that the dimensionless coupling $\lambda = Ng^2/(16\sqrt{v_1 v_2})$ is irrelevant around the Gaussian (non-interacting) fixed point, and thus justifies our perturbative calculations.

The RG flows for the ratio r_l and the tilting parameter $|w_l|$ are shown in Figs. 2 and 3, respectively. We see

that although both v_{1l} and v_{2l} increase at low energies, the rate of change of v_{2l} is faster than that of v_{1l} so that the ratio r_l decreases at low energies. Therefore, even if we take $v_1 = v_2$, $r_l \neq 1$ at $l > 0$. This is different from type-I Dirac fermions where $r_l = 1$ if $v_1 = v_2$. On the other hand, the value of $|w_l|$ always increases at low energies. This implies the stability of type-II Dirac fermions against weak Coulomb repulsions. Our result is distinct from the conclusion in Ref. 36.

IV. THERMODYNAMICS AT LOW TEMPERATURES OR SMALL DENSITIES

Now we are in a position to extract the temperature or density dependence of various thermodynamic response functions at low temperatures or small densities with the help of the RG equations, following the method proposed in Ref. 33.

Before doing it, we have to determine the RG flows of the temperature T and the chemical potential μ . At finite temperature, we find that

$$\tau \rightarrow s\tau,$$

according to the rescaling of p_0 . Hence, we get $(T')^{-1} = s^{-1}T^{-1}$ or

$$\frac{dT_l}{dl} = T_l. \quad (22)$$

The solution of Eq. (22) is $T_l = Te^l$.

To extract the scaling equation for μ , we add the term

$$-\mu \int_X \rho(X) = -\mu \sum_{\xi, \sigma} \int_P \tilde{\psi}_{\xi\sigma}^\dagger(P) \tilde{\psi}_{\xi\sigma}(P),$$

to the action. By integrating out the fast modes, this term becomes

$$-\frac{\mu}{v_1 v_2} \sum_{\xi, \sigma} \int_{-\infty}^{+\infty} \frac{dp_0}{2\pi} \int_{\Lambda/s} \frac{d^2 \tilde{p}}{(2\pi)^2} \tilde{\psi}_{\xi\sigma}^\dagger(P) \tilde{\psi}_{\xi\sigma}(P),$$

to the one-loop order. Performing the rescaling of E , θ , p_0 , and $\tilde{\psi}_{\xi\sigma}$, we find that

$$-\frac{\mu}{v_1 v_2} \sum_{\xi, \sigma} \int_{-\infty}^{+\infty} \frac{dp_0}{2\pi} \int_{\Lambda/s} \frac{d^2 \tilde{p}}{(2\pi)^2} \tilde{\psi}_{\xi\sigma}^\dagger(P) \tilde{\psi}_{\xi\sigma}(P) \\ = -\frac{s\mu}{v_1 v_2} \sum_{\xi, \sigma} \int_{-\infty}^{+\infty} \frac{dp_0}{2\pi} \int_{\Lambda} \frac{d^2 \tilde{p}}{(2\pi)^2} \tilde{\psi}_{\xi\sigma}^\dagger(P) \tilde{\psi}_{\xi\sigma}(P) \\ = -s\mu \sum_{\xi, \sigma} \int_P \tilde{\psi}_{\xi\sigma}^\dagger(P) \tilde{\psi}_{\xi\sigma}(P).$$

That is, $\mu' = s\mu$ or

$$\frac{d\mu_l}{dl} = \mu_l. \quad (23)$$

The solution of Eq. (23) is $\mu_l = \mu e^l$.

The first physical quantity we would like to study is the isothermal compressibility κ , which is defined as $\kappa = (\partial n / \partial \mu)_T$ where n is the average density of electrons. Since n is a physical quantity, upon renormalization, we find that

$$n(T, \mu, v_1, v_2, w, g^2) = s^{-2} n(T_l, \mu_l, v_{1l}, v_{2l}, w_l, g^2), \quad (24)$$

where $s = e^l$. We may regard $n(T_l, \mu_l, v_{1l}, v_{2l}, w_l, g^2)$ as the average density of the renormalized system where the effective coupling λ_l is small and the effective temperature T_l is high. With an appropriated choice for the renormalization scale l , we can put the renormalized theory into a regime in which the calculation becomes simple.

From Eq. (24) and the solutions of Eqs. (22) and (23), we find that $\kappa = s^{-1} \kappa_l$. We first consider the case with $\mu = 0$, and run the RG flow to the scale $l = l_*$ such that $T_{l_*} = D$ where D is the bandwidth which is the UV cutoff in energies for the model we use to describe the Dirac fermions. From the solution of Eq. (22), we have $l_* = \ln(D/T)$. In terms of this expression, we get $\kappa = e^{-l_*} \kappa_*$ where $A_* = A(l_*)$ denotes the renormalized variable at scale $l = l_*$. Since the effective coupling λ_l is irrelevant, we may replace k_* by the result of non-interacting fermions.

For type-I Dirac fermions, we have

$$\begin{aligned} \kappa_*(\mu = 0) &= \frac{(4 \ln 2) T_*}{\pi v_*^2 (1 - w_*^2)^{3/2}} \\ &= \frac{(4 \ln 2) D [1 + \frac{\lambda}{4} \ln(D/T)]^{-2}}{\pi v^2 \{1 - w^2 / [1 + \frac{\lambda}{4} \ln(D/T)]^2\}^{3/2}}. \end{aligned}$$

As a result, we get

$$\kappa(T) = \frac{(4 \ln 2) T [1 + \frac{\lambda}{4} \ln(D/T)]^{-2}}{\pi v^2 \{1 - w^2 / [1 + \frac{\lambda}{4} \ln(D/T)]^2\}^{3/2}}. \quad (25)$$

Equation (25) reduces to the one for graphene when $w = 0$ ³³. It indicates that the compressibility at given temperature is enhanced due to a nonzero tilting parameter. On the other hand, for type-II Dirac fermions, we have

$$\kappa_*(\mu = 0) = \frac{D e^{l_*}}{\pi^2 v_{1*} v_{2*} \tilde{w}_*},$$

leading to

$$\kappa(T) = \frac{D}{\pi^2 v_{1*} v_{2*} \tilde{w}_*}. \quad (26)$$

Figure 4 exhibits temperature dependence of κ^{-1} in units of κ_0^{-1} for both types of Dirac fermions, i.e.,

$$\frac{\kappa}{\kappa_0} = \frac{T/T_0}{[1 + \frac{\lambda}{4} \ln(T_0/T)]^2} \left\{ \frac{1 - w^2}{1 - w^2 / [1 + \frac{\lambda}{4} \ln(T_0/T)]^2} \right\}^{\frac{3}{2}},$$

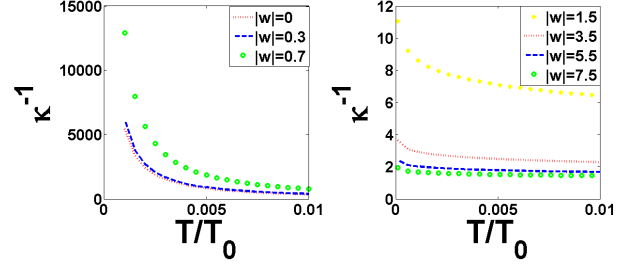


FIG. 4: $\kappa^{-1} = (\partial \mu / \partial n)_T$ at $\mu = 0$, in units of κ_0^{-1} , as a function of T/T_0 for type-I Dirac fermions (left) and type-II Dirac fermions (right), where κ_0 is the compressibility at $T = T_0 = D/k_B$. In both diagrams, we take $v_1 = v_2 = 1.3g^2/(4\pi)$.

for type-I Dirac fermions, and

$$\frac{\kappa}{\kappa_0} = \frac{v_1 v_2 \tilde{w}}{v_{1*} v_{2*} \tilde{w}_*},$$

for type-II Dirac fermions, where

$$\kappa_0 = \begin{cases} \frac{(4 \ln 2) T_0}{\pi v^2 (1 - w^2)^{3/2}} & \text{type-I} \\ \frac{D}{\pi^2 v_1 v_2 \tilde{w}} & \text{type-II} \end{cases},$$

is the compressibility at $T = T_0 = D/k_B$. We see that for both types of Dirac fermions, the compressibility at low temperatures is suppressed by the Coulomb interaction through the enhancement of the velocities. In particular, the compressibility is a constant for non-interacting type-II Dirac fermions. Hence, the behavior of $\kappa(T)$ at low temperatures deviates from the one of non-interacting fermions indicates the effect of Coulomb interactions.

Next, we consider the case with $T = 0$, and run the RG flow to the scale $l = l_*$ such that $|\mu_*| = D$, leading to $l_* = \ln(D/|\mu|)$. For type-I Dirac fermions, we have

$$\begin{aligned} n_*(T = 0) &= \frac{|\mu_*| \mu_*}{\pi v_*^2 (1 - w_*^2)^{3/2}} \\ &= \frac{\text{sgn}(\mu) D^2 [1 + \frac{\lambda}{4} \ln(D/|\mu|)]^{-2}}{\pi v^2 \{1 - w^2 / [1 + \frac{\lambda}{4} \ln(D/|\mu|)]^2\}^{3/2}}, \end{aligned}$$

which leads to

$$n(\mu) = \frac{|\mu| \mu [1 + \frac{\lambda}{4} \ln(D/|\mu|)]^{-2}}{\pi v^2 \{1 - w^2 / [1 + \frac{\lambda}{4} \ln(D/|\mu|)]^2\}^{3/2}}, \quad (27)$$

and $\kappa(\mu) \approx 2n(\mu)/\mu$. From Eq. (27), we find that

$$\begin{aligned} |\mu| &\approx \sqrt{\pi v^2 |n|} \left[1 + \frac{\lambda}{8} \ln \left(\frac{n_0}{|n|} \right) \right] \\ &\times \left\{ 1 - \frac{w^2}{[1 + \frac{\lambda}{8} \ln(n_0/|n|)]^2} \right\}^{3/4}, \end{aligned}$$

where $n_0 = D^2 / [\pi v^2 (1 - w^2)^{3/2}]$, and thus we obtain

$$\kappa(n) = \frac{2\sqrt{|n|/\pi} [1 + \frac{\lambda}{8} \ln(n_0/|n|)]^{-1}}{v \{1 - w^2 / [1 + \frac{\lambda}{8} \ln(n_0/|n|)]^2\}^{3/4}}. \quad (28)$$

When $w = 0$, Eqs. (27) and (28) reduce to those for graphene³³.

On the other hand, for type-II Dirac fermions, we have

$$n_*(T=0) = \frac{De^{l_*}\mu_*}{\pi^2 v_{1*} v_{2*} \tilde{w}_*} = \frac{D^3/\mu}{\pi^2 v_{1*} v_{2*} \tilde{w}_*},$$

$$\kappa_*(T=0) = \frac{De^{l_*}}{\pi^2 v_{1*} v_{2*} \tilde{w}_*} = \frac{D^2/|\mu|}{\pi^2 v_{1*} v_{2*} \tilde{w}_*}.$$

Hence, we get

$$n(\mu) = \frac{D\mu}{\pi^2 v_{1*} v_{2*} \tilde{w}_*}, \quad (29)$$

and

$$\kappa(\mu) = \frac{D}{\pi^2 v_{1*} v_{2*} \tilde{w}_*}.$$

From Eq. (29), we find that $|\mu| = \pi^2 v_{1*} v_{2*} \tilde{w}_* |n|/D$. Substituting this expression into $\kappa(\mu)$, we obtain

$$\kappa(n) = \frac{D}{\pi^2 v_{1*} v_{2*} \tilde{w}_*}, \quad (30)$$

where $l_* = \ln(n_0/|n|)$ and $n_0 = D^2/(\pi^2 v_{1*} v_{2*} \tilde{w}_*)$.

Now we determine the temperature dependence of the specific heat at constant volume, which can be extracted from the free energy density $f(T, \mu, v_1, v_2, w, g^2)$ through the relation $c(T) = -T\partial^2 f/\partial T^2$. Upon renormalization, we find that

$$f(T, \mu, v_1, v_2, w, g^2) = s^{-3} f(T_l, \mu_l, v_{1l}, v_{2l}, w_l, g^2). \quad (31)$$

Hence, we get $c(T) = e^{-2l_*} c_*$ where $l_* = \ln(D/T)$.

For type-I Dirac fermions, we have

$$c_* = \frac{18\zeta(3)T_*^2}{\pi v_*^2(1-w_*^2)^{3/2}} = \frac{18\zeta(3)D^2}{\pi v_*^2(1-w_*^2)^{3/2}},$$

which leads to

$$c(T) = \frac{18\zeta(3)T^2[1 + \frac{\lambda}{4} \ln(D/T)]^{-2}}{\pi v^2\{1 - w^2/[1 + \frac{\lambda}{4} \ln(D/T)]^2\}^{3/2}}. \quad (32)$$

Equation (32) reduces to the one for graphene when $w = 0$ ³³. On the other hand, for type-II Dirac fermions, we have

$$c_* = \frac{De^{l_*}T_*}{2v_{1*}v_{2*}\tilde{w}_*} = \frac{D^3/T}{2v_{1*}v_{2*}\tilde{w}_*},$$

which results in

$$c(T) = \frac{DT}{2v_{1*}v_{2*}\tilde{w}_*}. \quad (33)$$

We have to emphasize that the specific heat for type-II Dirac fermions at low temperatures is not linear in T because v_{1*} , v_{2*} , and \tilde{w}_* are functions of T . This deviation from the linear T behavior suggests the effect of Coulomb interactions.

V. SCREENING OF THE COULOMB POTENTIAL

One may wonder whether or not the above RG flows we obtained are cut at low energies due to the screening of the long range Coulomb interaction. To answer this question, we compute the vacuum polarization $\Pi(Q)$ to the one-loop order, where the vacuum polarization is defined by the Dyson equation

$$D^{-1}(Q) = \mathcal{V}_0^{-1}(\mathbf{q}) + \Pi(Q). \quad (34)$$

In Eq. (34), $D(Q)$ is the full propagator of the ϕ field and $\mathcal{V}_0(\mathbf{q}) = \frac{g^2}{2|\mathbf{q}|}$ is the bare ϕ propagator as well as the Fourier transform of the bare Coulomb potential $V_0(\mathbf{r})$. The Fourier transform $\mathcal{V}_s(\mathbf{q})$ of the renormalized Coulomb potential is then given by $\mathcal{V}_s(\mathbf{q}) = D(0, \mathbf{q})$.

A. The screened Coulomb potential

As we have shown, our RG equations for type-I Dirac fermions are identical to those by regularizing the theory with a momentum cutoff. Hence, we may compute $\Pi(Q)$ in terms of dimensional regularization³², yielding

$$\Pi(Q) = \frac{N}{16v_1v_2} \sum_{\xi} \frac{\tilde{\mathbf{q}}^2}{\sqrt{(q_0 + i\xi w \tilde{q}_1)^2 + \tilde{\mathbf{q}}^2}}. \quad (35)$$

When $w = 0$, Eq. (35) reduces to the one for graphene³². On the other hand, for type-II Dirac fermions, we have to employ our parametrization for momenta [Eq. (13)]. An exact evaluation of $\Pi(Q)$ is difficult. Fortunately, to answer the question of screening, it suffices to determine $\Pi(0, \mathbf{q})$, and we find that for $v_1|q_1|, v_2|q_2| \ll D$

$$\Pi(0, \mathbf{q}) = 2\tilde{w}^2 B D(0) \frac{(w^2 + 1)r^2 q_1^2 + q_2^2}{(w^2 + 1)^2 r^2 q_1^2 - \tilde{w}^2 q_2^2}, \quad (36)$$

where D is the band width, $r = v_1/v_2$, $D(0) = \frac{ND}{4\pi^2 v_1 v_2 \tilde{w}}$ is the DOS at the Fermi level, and B is a nonuniversal constant. The details of the calculations are left to appendix B.

Equations (35) and (36) indicate that

$$\lim_{q_1 \rightarrow 0} \lim_{q_2 \rightarrow 0} \Pi(0, \mathbf{q}) \neq \lim_{q_2 \rightarrow 0} \lim_{q_1 \rightarrow 0} \Pi(0, \mathbf{q}),$$

for type-II Dirac fermions and type-I Dirac fermions with $w \neq 0$. This implies that $\mathbf{q} = 0$ is a singular point of $\Pi(0, \mathbf{q})$ as well as $\mathcal{V}_s(\mathbf{q})$.

For type-II Dirac fermions, we remove this singularity by summing the leading divergent diagrams, following the method employed in Ref. 37. Since this theory is renormalizable, this can be achieved by replacing w and r in Eq. (36) by the energy dependent functions w_l and r_l and scaling w_l and r_l to the energy scale

$\sqrt{\tilde{w}^2 v_1^2 q_1^2 + v_2^2 q_2^2}$. Thus, the polarization function becomes

$$\Pi(0, \mathbf{q}) = 2\tilde{w}_l^2 BD(0) \frac{(w_l^2 + 1)r_l^2 q_1^2 + q_2^2}{(w_l^2 + 1)^2 r_l^2 q_1^2 - \tilde{w}_l^2 q_2^2}. \quad (37)$$

As we have shown, $|w_l|$ is an increasing function of l , while r_l is a decreasing function of l . Moreover, the product $|w_l|r_l$ increases with increasing l . Hence, at low energies (corresponding to small momenta), we may take $|w_l| \gg 1$ such that Eq. (37) can be approximated as $\Pi(0, \mathbf{q}) \approx 2BD(0)$. In terms of this expression, $\mathcal{V}_s(\mathbf{q})$ becomes

$$\mathcal{V}_s(\mathbf{q}) = \frac{g^2/2}{q + q_{TF}}, \quad (38)$$

which holds for $q = |\mathbf{q}| \ll q_{TF}$, where $q_{TF} = BD(0)g^2$ is the Thomas-Fermi wavenumber. When $r \gg 1/q_{TF}$, the screened Coulomb potential $V_s(\mathbf{r})$ behaves like

$$V_s(\mathbf{r}) \approx \frac{e^2}{4\pi\epsilon q_{TF}^2 r^3}, \quad (39)$$

instead of the bare one $V_0(\mathbf{r}) \sim 1/r$. This indicates that the RG flow we have obtained holds only when the energy scale is much larger than $v_0 q_{TF}$, where we have taken $v_1 = v_0 = v_2$. On account of the renormalization of the Coulomb interaction, $D(0)$ is smaller than the value for non-interacting fermions, and thus we expect that our results for the compressibility and specific heat hold for a large temperature range. Notice that the anisotropy of the screened Coulomb potential due to tilting is removed at long distances.

B. Coulomb impurity

In terms of the above polarization function, we can also study the Coulomb impurity problem for tilted Dirac fermions. Consider an impurity of charge Ze located at the origin, where the charge carried by an electron is $-e$. The charge density induced by this impurity is given by

$$\rho_{\text{ind}}(\mathbf{r}) = \int \frac{d^2 q}{(2\pi)^2} \tilde{\rho}_{\text{ind}}(\mathbf{q}) e^{i\mathbf{q} \cdot \mathbf{r}},$$

where

$$\tilde{\rho}_{\text{ind}}(\mathbf{q}) = -Ze\Pi(0, \mathbf{q})\mathcal{V}_s(\mathbf{q}), \quad (40)$$

For type-II Dirac fermions, we employ Eq. (38) and get

$$\tilde{\rho}_{\text{ind}}(\mathbf{q}) = -\frac{q_{TF}}{q + q_{TF}} Ze, \quad (41)$$

which holds only for $q \ll q_{TF}$. The total induced charge Q_{ind} is then given by

$$Q_{\text{ind}} = \int d^2 r \rho_{\text{ind}}(\mathbf{r}) = \tilde{\rho}_{\text{ind}}(0) = -Ze,$$

which implies the complete screening of the impurity charge. The presence of a nonvanishing screening length $1/q_{TF}$ and the complete screening of the impurity charge rely on a nonzero DOS at the Fermi energy. In contrast with the usual FL with a finite Fermi momentum, for type-II Dirac fermions, we have to sum the leading divergent diagrams beyond the RPA approximation.

For type-I Dirac fermions, we obtain

$$\tilde{\rho}_{\text{ind}}(\mathbf{q}) = -\frac{\lambda Zeq}{\sqrt{(1-w^2)q_1^2 + q_2^2} + \lambda q}, \quad (42)$$

within the RPA approximation, where for simplicity we have set $v_1 = v = v_2$ and $\lambda = Ng^2/(16v)$. When $w \neq 0$, we find that

$$\lim_{q_1 \rightarrow 0} \lim_{q_2 \rightarrow 0} \tilde{\rho}_{\text{ind}}(\mathbf{q}) \neq \lim_{q_2 \rightarrow 0} \lim_{q_1 \rightarrow 0} \tilde{\rho}_{\text{ind}}(\mathbf{q}).$$

That is, $\mathbf{q} = 0$ is a singular point of $\tilde{\rho}_{\text{ind}}(\mathbf{q})$ when $w \neq 0$. This singularity can also be removed by summing the leading logarithmically divergent diagrams. This can be achieved by replacing λ and w by $\lambda(p)$ and $w(p)$ and scaling $\lambda(p)$ and $w(p)$ to the momentum scale $p = q$. As a result, we get

$$\tilde{\rho}_{\text{ind}}(\mathbf{q}) = -\frac{q\lambda(q)Ze}{\sqrt{[1-w^2(q)]q_1^2 + q_2^2} + q\lambda(q)}. \quad (43)$$

Since $w(0) = 0$ and $\lambda(0) = 0$, we conclude that $Q_{\text{ind}} = \tilde{\rho}_{\text{ind}}(0) = 0$. In other words, the presence of an ion only leads to charge redistribution: a fraction of Z charge is pushed from short distances (of order of lattice spacing) to longer distances, but none of the charge goes to infinity. This situation is similar to graphene³⁷.

VI. CONCLUSIONS AND DISCUSSIONS

In the present work, we study the effects of Coulomb interactions on the tilted Dirac fermions in 2D with the help of RG. For type-I Dirac fermions, our method leads to identical results to previous studies. For type-II Dirac fermions, however, we find that the Coulomb interaction helps to stabilize the type-II Dirac semimetals, in contrast with previous works. Since our approach is perturbative in nature, the results hold only in the weak-coupling regime. Although we focus on tilted Dirac fermions in 2D, the extension of our method to tilted Weyl fermions in 3D is straightforward. In fact, the parametrization of momenta is similar to Eqs. (12) or (13), except the introduction of an additional “angle” variable.

With the help of the RG equations, we can study thermodynamics of tilted Dirac fermions at low temperatures and/or small densities. In particular, we calculate the temperature or density dependence of the isothermal compressibility and specific heat for both types of Dirac fermions.

To answer the question of screening of the Coulomb potential, we compute the vacuum polarization at zero frequency to the one-loop order for both types of Dirac fermions. For type-II Dirac fermions, we obtain a finite screening length, leading to total screening of a charged impurity, similar to the usual FL. Such a conclusion is obtained within the RPA approximation for the usual FL. In contrast, for type-II Dirac fermions, we have to go beyond the RPA approximation by summing the leading divergent diagrams. Since the screening length is inversely proportional to the DOS at the Fermi level and the latter is suppressed by Coulomb interactions, the screening length is larger than the one from the estimate based on non-interacting fermions. This implies that our results on the temperature or density dependence of the isothermal compressibility and specific heat for type-II Dirac fermions hold for a large temperature range. As for type-I Dirac fermions, the results are similar to those for graphene after summing the leading logarithmically divergent diagrams. The only effect of $w \neq 0$ is that the induced charge density becomes anisotropic due to the breaking of rotational symmetry.

The major difference between our work and the previous ones is that we adopt the regularization scheme such that the RG transformation is to scale to the Fermi surface for both types of Dirac fermions. This is important, in particular, for type-II Dirac fermions since its Fermi surface is open. This point is also noticed by a recent work on tilted Weyl fermions in 3D³⁹.

Another possible way to study this problem properly is to work directly on the low-energy effective theory for the fermionic excitations near the Fermi surface, as was done in Ref. 36. However, the conclusions in that work are distinct from ours. In our opinion, this distinction may arise from the following reason. The dimensional regularization employed there is a Lorentz/rotational-invariant regularization scheme which treats the frequency p_0 , the momenta parallel (p_{\parallel}) and perpendicular (p_{\perp}) to the Fermi lines on equal footing. However, the role played by p_{\parallel} is to parametrize the location of points on the Fermi lines, as what our parameter θ does. Fermionic excitations with different values of p_{\parallel} , but the same value of p_{\perp} , must have the same energy. Hence, the scaling of p_{\parallel} under the RG transformations can not be the same as the one of p_{\perp} since p_{\perp} scales to zero while p_{\parallel} does not. Accordingly, the use of dimensional regularization here is problematic.

An interesting question to ask is whether or how does the inclusion of transverse gauge fluctuations³⁵ by using our approach modify the above results. For the type-I case, it was shown that the velocities of the Dirac fermions are renormalized toward the speed of light and the tilting parameter flows to zero. Therefore, the Lorentz symmetry is restored at low energies. The situation is more subtle for type-II Dirac fermions since when the tilting parameter $|w| > 1$, the Fermi surface is not point-like and type-II Dirac fermions is separated from type-I Dirac fermions by a quantum phase transition point. Due to this intrinsic breaking of the

Lorentz/rotational symmetry, there is a priori no reason to expect that the same restoration of Lorentz symmetry will occur in the type-II case. Moreover, previous studies on the FL with a closed Fermi surface in 2D, interacting with transverse U(1) gauge fields, suggests that the low-energy physics is controlled by an interacting fixed point^{40–44}. Since the fate of type-II Dirac fermions interacting with transverse U(1) gauge fields is a dynamical issue, we leave it for future study.

Acknowledgments

The works of Y.L. Lee and Y.-W. Lee are supported by the Ministry of Science and Technology, Taiwan, under the grant number MOST 106-2112-M-018-003 and MOST 106-2112-M-029-002, respectively.

Appendix A: The self-energy of tilted Dirac fermions

Here we present the derivation of the one-loop RG equations. As we have discussed, it suffices to compute the self-energy $\Sigma_{\xi}(K)$ of fermions. To proceed, we need the free propagator of fermions:

$$\begin{aligned} \langle \mathcal{T}_{\tau} \{ \psi_{\xi\alpha}(X_1) \psi_{\xi'\alpha'}^{\dagger}(X_2) \} \rangle \\ = \delta_{\xi\xi'} \delta_{\alpha\alpha'} \int_P e^{-ip_0(\tau_1 - \tau_2) + i\mathbf{p} \cdot (\mathbf{r}_1 - \mathbf{r}_2)} G_{\xi 0}(P), \end{aligned}$$

and the free propagator of the bosonic field ϕ :

$$\langle \mathcal{T}_{\tau} \{ \phi(X_1) \phi(X_2) \} \rangle = \int_P e^{-ip_0(\tau_1 - \tau_2) + i\mathbf{p} \cdot (\mathbf{r}_1 - \mathbf{r}_2)} D_0(\mathbf{p}),$$

where $D_0(\mathbf{p}) = \mathcal{V}_0(\mathbf{p}) = \frac{g^2}{2|\mathbf{p}|}$ and

$$G_{\xi 0}(P) = \frac{ip_0 - \xi w v_1 p_1 + \xi v_1 p_1 \sigma_1 + v_2 p_2 \sigma_2}{(p_0 + i\xi w v_1 p_1)^2 + v_1^2 p_1^2 + v_2^2 p_2^2}.$$

By integrating out the fast modes, the following term

$$\sum_{\xi, \alpha} \int_K \tilde{\psi}_{\xi\alpha}^{\dagger}(K) \Sigma_{\xi}(K) \tilde{\psi}_{\xi\alpha}(K),$$

will be generated in the action S . To the one-loop order, we have

$$\begin{aligned} \Sigma_{\xi}(K) &= (-1) \cdot \frac{1}{2!} \cdot (-i)^2 \cdot 2 \int_P G_{\xi 0}(P) D_0(\mathbf{k} - \mathbf{p}) \\ &= \frac{g^2}{2} \int_P \frac{ip_0 - \xi w v_1 p_1 + \xi v_1 p_1 \sigma_1 + v_2 p_2 \sigma_2}{|\mathbf{k} - \mathbf{p}| [(p_0 + i\xi w v_1 p_1)^2 + v_1^2 p_1^2 + v_2^2 p_2^2]} \\ &= \Sigma_{\xi 0}(\mathbf{k}) \sigma_0 + \Sigma_{\xi 1}(\mathbf{k}) \sigma_1 + \Sigma_{\xi 2}(\mathbf{k}) \sigma_2, \end{aligned}$$

where σ_0 is the 2×2 unit matrix,

$$\begin{aligned}\Sigma_{\xi 0}(\mathbf{k}) &= \frac{ig^2}{2v_1v_2} \int_{\mathcal{D}} \frac{d^2\tilde{p}}{(2\pi)^2} \frac{1}{\sqrt{\sum_{a=1,2}(k_a - \tilde{p}_a/v_a)^2}} \\ &\quad \times \int_{-\infty}^{+\infty} \frac{dp_0}{2\pi} \frac{p_0 + i\xi w \tilde{p}_1}{(p_0 + i\xi w \tilde{p}_1)^2 + \tilde{\mathbf{p}}^2} \\ &= \frac{g^2}{8v_1v_2} \int_{\mathcal{D}} \frac{d^2\tilde{p}}{(2\pi)^2} \frac{\text{sgn}[\epsilon_+(\mathbf{p})] + \text{sgn}[\epsilon_-(\mathbf{p})]}{\sqrt{\sum_{a=1,2}(k_a - \tilde{p}_a/v_a)^2}},\end{aligned}$$

and

$$\begin{aligned}\Sigma_{\xi 1}(\mathbf{k}) &= \frac{\xi g^2}{2v_1v_2} \int_{\mathcal{D}} \frac{d^2\tilde{p}}{(2\pi)^2} \frac{\tilde{p}_1}{\sqrt{\sum_{a=1,2}(k_a - \tilde{p}_a/v_a)^2}} \\ &\quad \times \int_{-\infty}^{+\infty} \frac{dp_0}{2\pi} \frac{1}{(p_0 + i\xi w \tilde{p}_1)^2 + \tilde{\mathbf{p}}^2} \\ &= \frac{\xi g^2}{8v_1v_2} \int_{\mathcal{D}} \frac{d^2\tilde{p}}{(2\pi)^2} \frac{\tilde{p}_1[\text{sgn}(\epsilon_+(\mathbf{p})) - \text{sgn}(\epsilon_-(\mathbf{p}))]}{\tilde{p}\sqrt{\sum_{a=1,2}(k_a - \tilde{p}_a/v_a)^2}}, \\ \Sigma_{\xi 2}(\mathbf{k}) &= \frac{g^2}{2v_1v_2} \int_{\mathcal{D}} \frac{d^2\tilde{p}}{(2\pi)^2} \frac{\tilde{p}_2}{\sqrt{\sum_{a=1,2}(k_a - \tilde{p}_a/v_a)^2}} \\ &\quad \times \int_{-\infty}^{+\infty} \frac{dp_0}{2\pi} \frac{1}{(p_0 + i\xi w \tilde{p}_1)^2 + \tilde{\mathbf{p}}^2} \\ &= \frac{g^2}{8v_1v_2} \int_{\mathcal{D}} \frac{d^2\tilde{p}}{(2\pi)^2} \frac{\tilde{p}_2[\text{sgn}(\epsilon_+(\mathbf{p})) - \text{sgn}(\epsilon_-(\mathbf{p}))]}{\tilde{p}\sqrt{\sum_{a=1,2}(k_a - \tilde{p}_a/v_a)^2}}.\end{aligned}$$

In the above, \mathcal{D} is the energy shell in the range $\Lambda/s < |E| < \Lambda$.

1. Type-I Dirac fermions

We first consider type-I Dirac fermions. In this case, $\epsilon_+(\mathbf{p}) > 0$ and $\epsilon_-(\mathbf{p}) < 0$ as long as $E \neq 0$. Thus, the above expressions reduce to

$$\begin{aligned}\Sigma_{\xi 1}(\mathbf{k}) &= \frac{\xi g^2}{4v_1v_2} \int_{\mathcal{D}} \frac{d^2\tilde{p}}{(2\pi)^2} \frac{\tilde{p}_1}{\tilde{p}\sqrt{\sum_{a=1,2}(k_a - \tilde{p}_a/v_a)^2}}, \\ \Sigma_{\xi 2}(\mathbf{k}) &= \frac{g^2}{4v_1v_2} \int_{\mathcal{D}} \frac{d^2\tilde{p}}{(2\pi)^2} \frac{\tilde{p}_2}{\tilde{p}\sqrt{\sum_{a=1,2}(k_a - \tilde{p}_a/v_a)^2}}, \\ \Sigma_{\xi 0}(\mathbf{k}) &= 0.\end{aligned}$$

To proceed, we expand $\Sigma_{\xi a}(\mathbf{k})$ with $a = 1, 2$ to the linear orders in \mathbf{k} :

$$\Sigma_{\xi a}(\mathbf{k}) = \Sigma_{\xi a}^{(0)} + \sum_{i=1,2} \Sigma_{\xi a}^{(i)} k_i + O(k_i^2),$$

where

$$\begin{aligned}\Sigma_{\xi 1}^{(0)} &= \frac{\xi g^2}{4v_1^2v_2} \int_{\mathcal{D}} \frac{d^2\tilde{p}}{(2\pi)^2} \frac{\tilde{p}_1}{\tilde{p}\sqrt{(\tilde{p}_1/v_1)^2 + (\tilde{p}_2/v_2)^2}} \\ &= 0, \\ \Sigma_{\xi 2}^{(0)} &= \frac{\xi g^2}{4v_1^2v_2} \int_{\mathcal{D}} \frac{d^2\tilde{p}}{(2\pi)^2} \frac{\tilde{p}_2}{\tilde{p}\sqrt{(\tilde{p}_1/v_1)^2 + (\tilde{p}_2/v_2)^2}} \\ &= 0, \\ \Sigma_{\xi 1}^{(1)} &= \frac{\xi g^2}{4v_1^2v_2} \int_{\mathcal{D}} \frac{d^2\tilde{p}}{(2\pi)^2} \frac{\tilde{p}_1^2}{\tilde{p}[(\tilde{p}_1/v_1)^2 + (\tilde{p}_2/v_2)^2]^{3/2}}, \\ \Sigma_{\xi 1}^{(2)} &= \frac{\xi g^2}{4v_1v_2^2} \int_{\mathcal{D}} \frac{d^2\tilde{p}}{(2\pi)^2} \frac{\tilde{p}_1\tilde{p}_2}{\tilde{p}[(\tilde{p}_1/v_1)^2 + (\tilde{p}_2/v_2)^2]^{3/2}} \\ &= 0, \\ \Sigma_{\xi 2}^{(1)} &= \frac{g^2}{4v_1^2v_2} \int_{\mathcal{D}} \frac{d^2\tilde{p}}{(2\pi)^2} \frac{\tilde{p}_1\tilde{p}_2}{\tilde{p}[(\tilde{p}_1/v_1)^2 + (\tilde{p}_2/v_2)^2]^{3/2}} \\ &= 0, \\ \Sigma_{\xi 2}^{(2)} &= \frac{g^2}{4v_1v_2^2} \int_{\mathcal{D}} \frac{d^2\tilde{p}}{(2\pi)^2} \frac{\tilde{p}_2^2}{\tilde{p}[(\tilde{p}_1/v_1)^2 + (\tilde{p}_2/v_2)^2]^{3/2}}.\end{aligned}$$

$\Sigma_{\xi 1}^{(2)} = 0 = \Sigma_{\xi 2}^{(0)} = \Sigma_{\xi 2}^{(1)}$ because \mathcal{D} is symmetric under the reflection $\tilde{p}_2 \rightarrow -\tilde{p}_2$, while the integrands are odd functions of \tilde{p}_2 . On the other hand, $\Sigma_{\xi 1}^{(0)} = 0$ by an explicit calculation. The renormalized velocities v'_1 and v'_2 are then given by

$$v'_1 = v_1 + \xi \Sigma_{\xi 1}^{(1)}, \quad v'_2 = v_2 + \Sigma_{\xi 2}^{(2)}.$$

For simplicity, we consider $v_1 = v_2$, and we have

$$\begin{aligned}\Sigma_{\xi 1}^{(1)} &= \frac{\xi \sqrt{1-w^2} g^2}{32\pi^2} \int_{\Lambda/s}^{\Lambda} \frac{dE}{E} \int_0^{2\pi} \frac{(w - \xi \cos \theta)^2 d\theta}{(1 - \xi w \cos \theta)^3} \\ &\quad + \frac{\xi \sqrt{1-w^2} g^2}{32\pi^2} \int_{-\Lambda}^{-\Lambda/s} \frac{dE}{|E|} \int_0^{2\pi} \frac{(w + \xi \cos \theta)^2 d\theta}{(1 + \xi w \cos \theta)^3} \\ &= \frac{\xi g^2 l}{16\pi},\end{aligned}$$

and

$$\begin{aligned}\Sigma_{\xi 2}^{(2)} &= \frac{(1-w^2)^{3/2} g^2}{32\pi^2} \int_{\Lambda/s}^{\Lambda} \frac{dE}{E} \int_0^{2\pi} \frac{\sin^2 \theta d\theta}{(1 - \xi w \cos \theta)^3} \\ &\quad + \frac{(1-w^2)^{3/2} g^2}{32\pi^2} \int_{-\Lambda}^{-\Lambda/s} \frac{dE}{|E|} \int_0^{2\pi} \frac{\sin^2 \theta d\theta}{(1 + \xi w \cos \theta)^3} \\ &= \frac{g^2 l}{16\pi}.\end{aligned}$$

As a result, the renormalized velocity to the one-loop order is given by

$$v' = v + \frac{g^2 l}{16\pi},$$

which gives the RG equation for v in Eq. (18). On the other hand, wv_1 is not renormalized to the one-loop order because $\Sigma_{\xi 0} = 0$. Thus, we get

$$(wv_1)' = wv_1,$$

which leads to the RG equation for wv in Eq. (18).

2. Type-II Dirac fermions

Next, we consider type-II Dirac fermions. In terms of the parametrization (13), we find that

$$\begin{aligned}\text{sgn}(\epsilon_+) &= \text{sgn}(E) + 2\Theta(\pm\eta_w\xi)\Theta(-E)\Theta(|\theta| - \ln|w|) , \\ \text{sgn}(\epsilon_-) &= \text{sgn}(E) - 2\Theta(\mp\eta_w\xi)\Theta(E)\Theta(|\theta| - \ln|w|) ,\end{aligned}$$

where the upper and the lower signs correspond to the right and the left branches of the hyperbola, respectively. To compute the renormalization of various parameters in the action, we expand $\Sigma_{\xi\mu}(\mathbf{k})$ with $\mu = 0, 1, 2$ to the linear orders in \mathbf{k} :

$$\Sigma_{\xi\mu}(\mathbf{k}) = \Sigma_{\xi\mu}^{(0)} + \sum_{i=1,2} \Sigma_{\xi\mu}^{(i)} k_i + O(k_i^2) ,$$

Among these terms, $\Sigma_{\xi 0}^{(2)} = 0 = \Sigma_{\xi 1}^{(2)} = \Sigma_{\xi 2}^{(2)} = \Sigma_{\xi 2}^{(1)}$ because the integration domain is symmetric under the reflection $\tilde{p}_2 \rightarrow -\tilde{p}_2$, while the integrand is an odd function of \tilde{p}_2 . On the other hand, $\Sigma_{\xi 0}^{(0)} = 0 = \Sigma_{\xi 1}^{(0)}$ by explicit calculations. Thus, the nonvanishing terms are

$$\begin{aligned}\Sigma_{\xi 0}^{(1)} &= \frac{g^2}{32\pi^2 v_1^2 v_2} \int_{\mathcal{D}} d^2 \tilde{p} \frac{\tilde{p}_1 [\text{sgn}(\epsilon_+) + \text{sgn}(\epsilon_-)]}{[(\tilde{p}_1/v_1)^2 + (\tilde{p}_2/v_2)^2]^{3/2}} , \\ \Sigma_{\xi 1}^{(1)} &= \frac{\xi g^2}{32\pi^2 v_1^2 v_2} \int_{\mathcal{D}} d^2 \tilde{p} \frac{\tilde{p}_1^2 [\text{sgn}(\epsilon_+) - \text{sgn}(\epsilon_-)]}{\tilde{p} [(\tilde{p}_1/v_1)^2 + (\tilde{p}_2/v_2)^2]^{3/2}} , \\ \Sigma_{\xi 2}^{(2)} &= \frac{g^2}{32\pi^2 v_1 v_2^2} \int_{\mathcal{D}} d^2 \tilde{p} \frac{\tilde{p}_2^2 [\text{sgn}(\epsilon_+) - \text{sgn}(\epsilon_-)]}{\tilde{p} [(\tilde{p}_1/v_1)^2 + (\tilde{p}_2/v_2)^2]^{3/2}} .\end{aligned}$$

The renormalized values of wv_1 , v_1 , and v_2 to the one-loop order are then given by

$$\begin{aligned}(wv_1)' &= wv_1 + \xi \Sigma_{\xi 0}^{(1)} , \\ v_1' &= v_1 + \xi \Sigma_{\xi 1}^{(1)} , \\ v_2' &= v_2 + \Sigma_{\xi 2}^{(2)} .\end{aligned}$$

In terms of Eqs. (13) and (15), we find that

$$\begin{aligned}(wv_1)' &= wv_1 + \frac{\eta_w \tilde{w} g^2 r l}{8\pi^2} (J_1 - J_2) , \\ v_1' &= v_1 + \frac{\tilde{w} g^2 r l}{8\pi^2} M_1 , \\ v_2' &= v_2 + \frac{\tilde{w}^3 g^2 r^2 l}{8\pi^2} M_2 ,\end{aligned}$$

where

$$\begin{aligned}J_1 &= \int_0^{+\infty} d\theta \left\{ \frac{(|w| \cosh \theta + 1)(|w| + \cosh \theta)}{[(|w| + \cosh \theta)^2 + r^2 \tilde{w}^2 \sinh^2 \theta]^{3/2}} \right. \\ &\quad \left. + \frac{(|w| \cosh \theta - 1)(|w| - \cosh \theta)}{[(|w| - \cosh \theta)^2 + r^2 \tilde{w}^2 \sinh^2 \theta]^{3/2}} \right\} , \\ J_2 &= \int_{\ln|w|}^{+\infty} d\theta \frac{(|w| \cosh \theta - 1)(|w| - \cosh \theta)}{[(|w| - \cosh \theta)^2 + r^2 \tilde{w}^2 \sinh^2 \theta]^{3/2}} .\end{aligned}$$

while M_1 and M_2 are defined in Sec. III. From the above equations, we obtain Eqs. (19) – (21) with the function $\mathcal{N} = J_1 - J_2 - |w|M_1$.

Appendix B: The vacuum polarization

Here we compute the vacuum polarization to the one-loop order, which is given by

$$\begin{aligned}\Pi(Q) &= (-2) \cdot \frac{1}{2!} \cdot (-i)^2 \cdot (-1) \cdot N \sum_{\xi} \int_P \text{tr}[G_{\xi 0}(P) G_{\xi 0}(P + Q)] \\ &= \frac{2N}{v_1 v_2} \sum_{\xi} \int \frac{d^2 \tilde{p}}{(2\pi)^2} \int_{-\infty}^{+\infty} \frac{dp_0}{2\pi} \frac{(p_0 + i\xi w \tilde{p}_1)[p_0 + q_0 + i\xi w(\tilde{p}_1 + \tilde{q}_1)] - \tilde{\mathbf{p}} \cdot (\tilde{\mathbf{p}} + \tilde{\mathbf{q}})}{[p_0 + i\epsilon_+(\mathbf{p})][p_0 + i\epsilon_-(\mathbf{p})][p_0 + q_0 + i\epsilon_+(\mathbf{p} + \mathbf{q})][p_0 + q_0 + i\epsilon_-(\mathbf{p} + \mathbf{q})]} ,\end{aligned}$$

where $\tilde{\mathbf{q}} = (v_1 q_1, v_2 q_2)$.

For type-I Dirac fermions, we employ the Feynmann parametrization

$$\frac{1}{ab} = \int_0^1 \frac{dx}{[ax + b(1-x)]^2} ,$$

and write $\Pi(Q)$ as

$$\begin{aligned}
\Pi(Q) &= \frac{2N}{v_1 v_2} \sum_{\xi} \int_0^1 dx \int_{-\infty}^{+\infty} \frac{d^3 P}{(2\pi)^3} \frac{(p_0 + i\xi w \tilde{p}_1)[p_0 + q_0 + i\xi w(\tilde{p}_1 + \tilde{q}_1)] - \tilde{\mathbf{p}} \cdot (\tilde{\mathbf{p}} + \tilde{\mathbf{q}})}{\{[(p_0 + i\xi w \tilde{p}_1)^2 + \tilde{\mathbf{p}}^2](1-x) + x[(p_0 + q_0 + i\xi w(\tilde{p}_1 + \tilde{q}_1))^2 + (\tilde{\mathbf{p}} + \tilde{\mathbf{q}})^2]\}^2} \\
&= \frac{2N}{v_1 v_2} \sum_{\xi} \int_0^1 dx \int_{-\infty}^{+\infty} \frac{d^3 P}{(2\pi)^3} \frac{(p_0 + i\xi w \tilde{p}_1)[p_0 + q_0 + i\xi w(\tilde{p}_1 + \tilde{q}_1)] - \tilde{\mathbf{p}} \cdot (\tilde{\mathbf{p}} + \tilde{\mathbf{q}})}{\{[p_0 + i\xi w \tilde{p}_1 + x(q_0 + i\xi w \tilde{q}_1)]^2 + (\tilde{\mathbf{p}} + x\tilde{\mathbf{q}})^2 + x(1-x)[(q_0 + i\xi w \tilde{q}_1)^2 + \tilde{\mathbf{q}}^2]\}^2} \\
&= \frac{2N}{v_1 v_2} \sum_{\xi} \int_0^1 dx \int_{-\infty}^{+\infty} \frac{d^3 P}{(2\pi)^3} \frac{1}{\{(p_0 + i\xi w \tilde{p}_1)^2 + \tilde{\mathbf{p}}^2 + x(1-x)[(q_0 + i\xi w \tilde{q}_1)^2 + \tilde{\mathbf{q}}^2]\}^2} \\
&\quad \times \{(p_0 + i\xi w \tilde{p}_1)^2 - \tilde{\mathbf{p}}^2 + (1-2x)[(p_0 + i\xi w \tilde{p}_1)(q_0 + i\xi w \tilde{q}_1) - \tilde{\mathbf{p}} \cdot \tilde{\mathbf{q}} - x(1-x)[(q_0 + i\xi w \tilde{q}_1)^2 - \tilde{\mathbf{q}}^2]\} \\
&= \frac{2N}{v_1 v_2} \sum_{\xi} \int_0^1 dx \int_{-\infty}^{+\infty} \frac{d^3 P}{(2\pi)^3} \frac{p_0^2 - \tilde{\mathbf{p}}^2 - x(1-x)[(q_0 + i\xi w \tilde{q}_1)^2 - \tilde{\mathbf{q}}^2]}{\{P^2 + x(1-x)[(q_0 + i\xi w \tilde{q}_1)^2 + \tilde{\mathbf{q}}^2]\}^2} \\
&= -\frac{2N}{v_1 v_2} \sum_{\xi} \int_0^1 dx \int_{-\infty}^{+\infty} \frac{d^3 P}{(2\pi)^3} \frac{P^2/3 + x(1-x)[(q_0 + i\xi w \tilde{q}_1)^2 - \tilde{\mathbf{q}}^2]}{\{P^2 + x(1-x)[(q_0 + i\xi w \tilde{q}_1)^2 + \tilde{\mathbf{q}}^2]\}^2},
\end{aligned}$$

where $d^3 P = dp_0 d^2 \tilde{\mathbf{p}}$ and $P^2 = p_0^2 + \tilde{\mathbf{p}}^2$. We regularize the momentum integral in terms of the dimensional regularization, yielding

$$\Pi(Q) = \frac{N}{2\pi v_1 v_2} \sum_{\xi} \frac{\tilde{\mathbf{q}}^2}{\sqrt{(q_0 + i\xi w \tilde{q}_1)^2 + \tilde{\mathbf{q}}^2}} \int_0^1 dx \sqrt{x(1-x)}.$$

Performing the x integral, we get Eq. (35).

For type-II Dirac fermions, we first perform the p_0 integral, yielding

$$\begin{aligned}
\Pi(Q) &= -\frac{2N}{v_1 v_2} \sum_{\xi} \int \frac{d^2 \tilde{\mathbf{p}}}{(2\pi)^2} \frac{\text{sgn}[\epsilon_{-}(\mathbf{p})][\tilde{p}(\xi w \tilde{q}_1 - i q_0) + \tilde{\mathbf{p}}^2 + \tilde{\mathbf{p}} \cdot (\tilde{\mathbf{p}} + \tilde{\mathbf{q}})]}{\tilde{p}[\epsilon_{+}(\mathbf{p} + \mathbf{q}) - \epsilon_{-}(\mathbf{p}) - i q_0][\epsilon_{-}(\mathbf{p} + \mathbf{q}) - \epsilon_{-}(\mathbf{p}) - i q_0]} \\
&\quad - \frac{2N}{v_1 v_2} \sum_{\xi} \int \frac{d^2 \tilde{\mathbf{p}}}{(2\pi)^2} \frac{\text{sgn}[\epsilon_{+}(\mathbf{p})][\tilde{p}(\xi w \tilde{q}_1 - i q_0) - \tilde{\mathbf{p}}^2 - \tilde{\mathbf{p}} \cdot (\tilde{\mathbf{p}} + \tilde{\mathbf{q}})]}{\tilde{p}[\epsilon_{+}(\mathbf{p} + \mathbf{q}) - \epsilon_{+}(\mathbf{p}) - i q_0][\epsilon_{-}(\mathbf{p} + \mathbf{q}) - \epsilon_{+}(\mathbf{p}) - i q_0]}.
\end{aligned}$$

It is straightforward to verify that $\Pi(q_0, 0) = 0$. On the other hand, $\Pi(0, \mathbf{q})$ can be written as

$$\begin{aligned}
\Pi(0, \mathbf{q}) &= -\frac{2N}{v_1 v_2} \sum_{\xi} \int \frac{d^2 \tilde{\mathbf{p}}}{(2\pi)^2} \frac{\text{sgn}[\epsilon_{-}(\mathbf{p})][\xi w \tilde{q}_1 \tilde{p} + \tilde{\mathbf{p}}^2 + \tilde{\mathbf{p}} \cdot (\tilde{\mathbf{p}} + \tilde{\mathbf{q}})]}{\tilde{p}(\xi w \tilde{q}_1 + |\tilde{\mathbf{p}} + \tilde{\mathbf{q}}| + \tilde{p})[\xi w \tilde{q}_1 - (|\tilde{\mathbf{p}} + \tilde{\mathbf{q}}| - \tilde{p})]} \\
&\quad - \frac{2N}{v_1 v_2} \sum_{\xi} \int \frac{d^2 \tilde{\mathbf{p}}}{(2\pi)^2} \frac{\text{sgn}[\epsilon_{+}(\mathbf{p})][\xi w \tilde{q}_1 \tilde{p} - \tilde{\mathbf{p}}^2 - \tilde{\mathbf{p}} \cdot (\tilde{\mathbf{p}} + \tilde{\mathbf{q}})]}{\tilde{p}[\xi w \tilde{q}_1 + (|\tilde{\mathbf{p}} + \tilde{\mathbf{q}}| - \tilde{p})][\xi w \tilde{q}_1 - (|\tilde{\mathbf{p}} + \tilde{\mathbf{q}}| + \tilde{p})]} \\
&= -\frac{N}{8\pi^2 v_1 v_2 \tilde{w}} [F_1(\mathbf{q}) - F_2(\mathbf{q})] - \frac{N}{4\pi^2 v_1 v_2 \tilde{w}^3} [F_3(\mathbf{q}) + F_4(\mathbf{q})].
\end{aligned}$$

where

$$\begin{aligned}
F_1(\mathbf{q}) &= \sum_{\xi} \int_{-\Lambda}^{\Lambda} dE \int_{-\infty}^{+\infty} d\theta \frac{[|w|(\xi w \cosh \theta + \eta_E) + (\eta_E \xi w + \cosh \theta)]\tilde{q}_1 + \tilde{w}\tilde{q}_2 \sinh \theta}{[|w|(\xi w \cosh \theta + \eta_E) - (\eta_E \xi w + \cosh \theta)]\tilde{q}_1 - \tilde{w}\tilde{q}_2 \sinh \theta + \frac{\tilde{w}^2}{2|E|}(\tilde{w}^2\tilde{q}_1^2 - \tilde{q}_2^2)} \\
&\quad \times [\operatorname{sgn}(E) - 2\Theta(-\eta_w \xi)\Theta(E)\Theta(|\theta| - \ln |w|)] \\
&\quad + \sum_{\xi} \int_{-\Lambda}^{\Lambda} dE \int_{-\infty}^{+\infty} d\theta \frac{[|w|(\xi w \cosh \theta - \eta_E) + (\eta_E \xi w - \cosh \theta)]\tilde{q}_1 + \tilde{w}\tilde{q}_2 \sinh \theta}{[|w|(\xi w \cosh \theta - \eta_E) - (\eta_E \xi w - \cosh \theta)]\tilde{q}_1 - \tilde{w}\tilde{q}_2 \sinh \theta + \frac{\tilde{w}^2}{2|E|}(\tilde{w}^2\tilde{q}_1^2 - \tilde{q}_2^2)} \\
&\quad \times [\operatorname{sgn}(E) - 2\Theta(\eta_w \xi)\Theta(E)\Theta(|\theta| - \ln |w|)] , \\
F_2(\mathbf{q}) &= \sum_{\xi} \int_{-\Lambda}^{\Lambda} dE \int_{-\infty}^{+\infty} d\theta \frac{[|w|(\xi w \cosh \theta + \eta_E) - (\eta_E \xi w + \cosh \theta)]\tilde{q}_1 - \tilde{w}\tilde{q}_2 \sinh \theta}{[|w|(\xi w \cosh \theta + \eta_E) + (\eta_E \xi w + \cosh \theta)]\tilde{q}_1 + \tilde{w}\tilde{q}_2 \sinh \theta - \frac{\tilde{w}^2}{2|E|}(\tilde{w}^2\tilde{q}_1^2 - \tilde{q}_2^2)} \\
&\quad \times [\operatorname{sgn}(E) + 2\Theta(\eta_w \xi)\Theta(-E)\Theta(|\theta| - \ln |w|)] \\
&\quad + \sum_{\xi} \int_{-\Lambda}^{\Lambda} dE \int_{-\infty}^{+\infty} d\theta \frac{[|w|(\xi w \cosh \theta - \eta_E) - (\eta_E \xi w - \cosh \theta)]\tilde{q}_1 - \tilde{w}\tilde{q}_2 \sinh \theta}{[|w|(\xi w \cosh \theta - \eta_E) + (\eta_E \xi w - \cosh \theta)]\tilde{q}_1 + \tilde{w}\tilde{q}_2 \sinh \theta - \frac{\tilde{w}^2}{2|E|}(\tilde{w}^2\tilde{q}_1^2 - \tilde{q}_2^2)} \\
&\quad \times [\operatorname{sgn}(E) + 2\Theta(-\eta_w \xi)\Theta(-E)\Theta(|\theta| - \ln |w|)] ,
\end{aligned}$$

and

$$\begin{aligned}
F_3(\mathbf{q}) &= \sum_{\xi} \int_{-\Lambda}^{\Lambda} dE \int_{-\infty}^{+\infty} d\theta \frac{|E|(|w| \cosh \theta + \eta_E \eta_w \xi)^2}{[|w|(\xi w \cosh \theta + \eta_E) - (\eta_E \xi w + \cosh \theta)]\tilde{q}_1 - \tilde{w}\tilde{q}_2 \sinh \theta + \frac{\tilde{w}^2}{2|E|}(\tilde{w}^2\tilde{q}_1^2 - \tilde{q}_2^2)} \\
&\quad \times [\operatorname{sgn}(E) - 2\Theta(-\eta_w \xi)\Theta(E)\Theta(|\theta| - \ln |w|)] \\
&\quad + \sum_{\xi} \int_{-\Lambda}^{\Lambda} dE \int_{-\infty}^{+\infty} d\theta \frac{|E|(|w| \cosh \theta - \eta_E \eta_w \xi)^2}{[|w|(\xi w \cosh \theta - \eta_E) - (\eta_E \xi w - \cosh \theta)]\tilde{q}_1 - \tilde{w}\tilde{q}_2 \sinh \theta + \frac{\tilde{w}^2}{2|E|}(\tilde{w}^2\tilde{q}_1^2 - \tilde{q}_2^2)} \\
&\quad \times [\operatorname{sgn}(E) - 2\Theta(\eta_w \xi)\Theta(E)\Theta(|\theta| - \ln |w|)] , \\
F_4(\mathbf{q}) &= \sum_{\xi} \int_{-\Lambda}^{\Lambda} dE \int_{-\infty}^{+\infty} d\theta \frac{|E|(|w| \cosh \theta + \eta_E \eta_w \xi)^2}{[|w|(\xi w \cosh \theta + \eta_E) + (\eta_E \xi w + \cosh \theta)]\tilde{q}_1 + \tilde{w}\tilde{q}_2 \sinh \theta - \frac{\tilde{w}^2}{2|E|}(\tilde{w}^2\tilde{q}_1^2 - \tilde{q}_2^2)} \\
&\quad \times [\operatorname{sgn}(E) + 2\Theta(\eta_w \xi)\Theta(-E)\Theta(|\theta| - \ln |w|)] \\
&\quad + \sum_{\xi} \int_{-\Lambda}^{\Lambda} dE \int_{-\infty}^{+\infty} d\theta \frac{|E|(|w| \cosh \theta - \eta_E \eta_w \xi)^2}{[|w|(\xi w \cosh \theta - \eta_E) + (\eta_E \xi w - \cosh \theta)]\tilde{q}_1 + \tilde{w}\tilde{q}_2 \sinh \theta - \frac{\tilde{w}^2}{2|E|}(\tilde{w}^2\tilde{q}_1^2 - \tilde{q}_2^2)} \\
&\quad \times [\operatorname{sgn}(E) + 2\Theta(-\eta_w \xi)\Theta(-E)\Theta(|\theta| - \ln |w|)] ,
\end{aligned}$$

where Λ is the UV cutoff in energies.

An exact evaluation of $\Pi(0, \mathbf{q})$ is difficult. Instead of doing it, we shall determine it for $v_1|q_1|, v_2|q_2| \ll D$. This can be done by calculating $\partial\Pi/\partial\Lambda$, yielding

$$\frac{\partial}{\partial\Lambda}\Pi_{\Lambda} = -\frac{N}{8\pi^2 v_1 v_2 \tilde{w}} \left[\frac{\partial}{\partial\Lambda} F_1(\mathbf{q}) - \frac{\partial}{\partial\Lambda} F_2(\mathbf{q}) \right] - \frac{N}{4\pi^2 v_1 v_2 \tilde{w}^3} \left[\frac{\partial}{\partial\Lambda} F_3(\mathbf{q}) + \frac{\partial}{\partial\Lambda} F_4(\mathbf{q}) \right] , \quad (\text{B1})$$

and

$$\frac{\partial}{\partial\Lambda} F_{1/2}(\mathbf{q}) = \mathcal{F}_{1/2}(\mathbf{q}) , \quad \frac{\partial}{\partial\Lambda} F_{3/4}(\mathbf{q}) = \Lambda \mathcal{F}_{3/4}(\mathbf{q}) ,$$

where Π_{Λ} is the vacuum polarization with the energy cutoff Λ ,

$$\begin{aligned}
\mathcal{F}_1(\mathbf{q}) &= \sum_{\xi} \int_{-\infty}^{+\infty} d\theta \frac{[|w|(\xi w \cosh \theta + 1) + (\xi w + \cosh \theta)]\tilde{q}_1 + \tilde{w}\tilde{q}_2 \sinh \theta}{[|w|(\xi w \cosh \theta + 1) - (\xi w + \cosh \theta)]\tilde{q}_1 - \tilde{w}\tilde{q}_2 \sinh \theta} [1 - 2\Theta(-\eta_w \xi)\Theta(|\theta| - \ln |w|)] \\
&\quad + \sum_{\xi} \int_{-\infty}^{+\infty} d\theta \frac{[|w|(\xi w \cosh \theta - 1) + (\xi w - \cosh \theta)]\tilde{q}_1 + \tilde{w}\tilde{q}_2 \sinh \theta}{[|w|(\xi w \cosh \theta - 1) - (\xi w - \cosh \theta)]\tilde{q}_1 - \tilde{w}\tilde{q}_2 \sinh \theta} [1 - 2\Theta(\eta_w \xi)\Theta(|\theta| - \ln |w|)] \\
&\quad - \sum_{\xi} \int_{-\infty}^{+\infty} d\theta \frac{[|w|(\xi w \cosh \theta - 1) - (\xi w - \cosh \theta)]\tilde{q}_1 + \tilde{w}\tilde{q}_2 \sinh \theta}{[|w|(\xi w \cosh \theta - 1) + (\xi w - \cosh \theta)]\tilde{q}_1 - \tilde{w}\tilde{q}_2 \sinh \theta} \\
&\quad - \sum_{\xi} \int_{-\infty}^{+\infty} d\theta \frac{[|w|(\xi w \cosh \theta + 1) - (\xi w + \cosh \theta)]\tilde{q}_1 + \tilde{w}\tilde{q}_2 \sinh \theta}{[|w|(\xi w \cosh \theta + 1) + (\xi w + \cosh \theta)]\tilde{q}_1 - \tilde{w}\tilde{q}_2 \sinh \theta} ,
\end{aligned}$$

$$\begin{aligned}
\mathcal{F}_2(\mathbf{q}) = & \sum_{\xi} \int_{-\infty}^{+\infty} d\theta \frac{[|w|(\xi w \cosh \theta + 1) - (\xi w + \cosh \theta)]\tilde{q}_1 - \tilde{w}\tilde{q}_2 \sinh \theta}{[|w|(\xi w \cosh \theta + 1) + (\xi w + \cosh \theta)]\tilde{q}_1 + \tilde{w}\tilde{q}_2 \sinh \theta} \\
& + \sum_{\xi} \int_{-\infty}^{+\infty} d\theta \frac{[|w|(\xi w \cosh \theta - 1) - (\xi w - \cosh \theta)]\tilde{q}_1 - \tilde{w}\tilde{q}_2 \sinh \theta}{[|w|(\xi w \cosh \theta - 1) + (\xi w - \cosh \theta)]\tilde{q}_1 + \tilde{w}\tilde{q}_2 \sinh \theta} \\
& + \sum_{\xi} \int_{-\infty}^{+\infty} d\theta \frac{[|w|(\xi w \cosh \theta - 1) + (\xi w - \cosh \theta)]\tilde{q}_1 - \tilde{w}\tilde{q}_2 \sinh \theta}{[|w|(\xi w \cosh \theta - 1) - (\xi w - \cosh \theta)]\tilde{q}_1 + \tilde{w}\tilde{q}_2 \sinh \theta} [-1 + 2\Theta(\eta_w \xi)\Theta(|\theta| - \ln |w|)] \\
& + \sum_{\xi} \int_{-\infty}^{+\infty} d\theta \frac{[|w|(\xi w \cosh \theta + 1) + (\xi w + \cosh \theta)]\tilde{q}_1 - \tilde{w}\tilde{q}_2 \sinh \theta}{[|w|(\xi w \cosh \theta + 1) - (\xi w + \cosh \theta)]\tilde{q}_1 + \tilde{w}\tilde{q}_2 \sinh \theta} [-1 + 2\Theta(-\eta_w \xi)\Theta(|\theta| - \ln |w|)] ,
\end{aligned}$$

$$\begin{aligned}
\mathcal{F}_3(\mathbf{q}) = & \sum_{\xi} \int_{-\infty}^{+\infty} d\theta \frac{(|w| \cosh \theta + \eta_w \xi)^2}{[|w|(\xi w \cosh \theta + 1) - (\xi w + \cosh \theta)]\tilde{q}_1 - \tilde{w}\tilde{q}_2 \sinh \theta} [1 - 2\Theta(-\eta_w \xi)\Theta(|\theta| - \ln |w|)] \\
& + \sum_{\xi} \int_{-\infty}^{+\infty} d\theta \frac{(|w| \cosh \theta - \eta_w \xi)^2}{[|w|(\xi w \cosh \theta - 1) - (\xi w - \cosh \theta)]\tilde{q}_1 - \tilde{w}\tilde{q}_2 \sinh \theta} [1 - 2\Theta(\eta_w \xi)\Theta(|\theta| - \ln |w|)] \\
& - \sum_{\xi} \int_{-\infty}^{+\infty} d\theta \frac{(|w| \cosh \theta - \eta_w \xi)^2}{[|w|(\xi w \cosh \theta - 1) + (\xi w - \cosh \theta)]\tilde{q}_1 - \tilde{w}\tilde{q}_2 \sinh \theta} \\
& - \sum_{\xi} \int_{-\infty}^{+\infty} d\theta \frac{(|w| \cosh \theta + \eta_w \xi)^2}{[|w|(\xi w \cosh \theta + 1) + (\xi w + \cosh \theta)]\tilde{q}_1 - \tilde{w}\tilde{q}_2 \sinh \theta} ,
\end{aligned}$$

and

$$\begin{aligned}
\mathcal{F}_4(\mathbf{q}) = & \sum_{\xi} \int_{-\infty}^{+\infty} d\theta \frac{(|w| \cosh \theta + \eta_w \xi)^2}{[|w|(\xi w \cosh \theta + 1) + (\xi w + \cosh \theta)]\tilde{q}_1 + \tilde{w}\tilde{q}_2 \sinh \theta} \\
& + \sum_{\xi} \int_{-\infty}^{+\infty} d\theta \frac{(|w| \cosh \theta - \eta_w \xi)^2}{[|w|(\xi w \cosh \theta - 1) + (\xi w - \cosh \theta)]\tilde{q}_1 + \tilde{w}\tilde{q}_2 \sinh \theta} \\
& + \sum_{\xi} \int_{-\infty}^{+\infty} d\theta \frac{(|w| \cosh \theta - \eta_w \xi)^2}{[|w|(\xi w \cosh \theta - 1) - (\xi w - \cosh \theta)]\tilde{q}_1 + \tilde{w}\tilde{q}_2 \sinh \theta} [-1 + 2\Theta(\eta_w \xi)\Theta(|\theta| - \ln |w|)] \\
& + \sum_{\xi} \int_{-\infty}^{+\infty} d\theta \frac{(|w| \cosh \theta + \eta_w \xi)^2}{[|w|(\xi w \cosh \theta + 1) - (\xi w + \cosh \theta)]\tilde{q}_1 + \tilde{w}\tilde{q}_2 \sinh \theta} [-1 + 2\Theta(-\eta_w \xi)\Theta(|\theta| - \ln |w|)] .
\end{aligned}$$

In the above, we have assumed that $|\tilde{q}_1|, |\tilde{q}_2| \ll \Lambda$. Explication calculations gives $\mathcal{F}_3(\mathbf{q}) + \mathcal{F}_4(\mathbf{q}) = 0$ and

$$\begin{aligned}
\mathcal{F}_1(\mathbf{q}) &= -\frac{8\tilde{w}^2[(w^2 + 1)\tilde{q}_1^2 + \tilde{q}_2^2]}{(w^2 + 1)^2\tilde{q}_1^2 - \tilde{w}^2\tilde{q}_2^2} \theta_{\Lambda} \\
&= -\mathcal{F}_2(\mathbf{q}) ,
\end{aligned}$$

where θ_{Λ} is the cutoff in θ , which is determined by the size of the first BZ. Collecting the above results and integrating Eq. (B1) from $\Lambda = 0$ to $\Lambda = D$, we obtain Eq. (36) with the nonuniversal constant $B = 4\theta_{\Lambda}$.

* Electronic address: ywlee@thu.edu.tw

† Electronic address: yllee@cc.ncue.edu.tw

¹ R. Shankar, Rev. Mod. Phys. **66**, 129 (1994).

² X.G. Wan, A.M. Turner, A. Vishwanath, and S.Y. Savrasov, Phys. Rev. B **83**, 205101 (2011).

³ A.A. Zyuzin and A.A. Burkov, Phys. Rev. B **86**, 115133 (2012).

⁴ Z. Wang and S.-C. Zhang, Phys. Rev. B **87**, 161107(R) (2013).

⁵ C.X. Liu, P. Ye, and X.-L. Qi, Phys. Rev. B **87**, 235306 (2013).

⁶ P. Goswami and S. Tewari, Phys. Rev. B **88**, 245107 (2013).

⁷ For a recent review, see P. Hosur and X.L. Qi, C. R.

- Physique **14**, 857 (2013).
- ⁸ C. Shekhar, A.K. Nayak, Y. Sun, M. Schmidt, M. Nicklas, I. Leermakers, U. Zeitler, Y. Skourski, J. Wosnitza, Z.K. Liu, Y.L. Chen, W. Schnelle, H. Borrmann, Y.R. Grin, C. Felser, and B.H. Yan, *Nat. Phys.* **11**, 645 (2015).
 - ⁹ B.Q. Lv, H.M. Weng, B.B. Fu, X.P. Wang, H. Miao, J. Ma, P. Richard, X.C. Huang, L.X. Zhao, G.F. Chen, Z. Fang, X. Dai, T. Qian, and H. Ding, *Phys. Rev. X* **5**, 031013 (2015).
 - ¹⁰ S.Y. Xu, I. Belopolski, N. Alidoust, M. Neupane, G. Bian, C.L. Zhang, R. Sankar, G.Q. Chang, Z.J. Yuan, C.C. Lee, S.M. Huang, H. Zheng, J. Ma, D.S. Sanchez, B.K. Wang, A. Bansil, F.C. Chou, P.P. Shibayev, H. Lin, S. Jia, and M.Z. Hasan, *Science* **349**, 613 (2015).
 - ¹¹ B.Q. Lv, N. Xu, H.M. Weng, J.Z. Ma, P. Richard, X.C. Huang, L.X. Zhao, G.F. Chen, C.E. Matt, F. Bisti, V.N. Strocov, J. Mesot, Z. Fang, X. Dai, T. Qian, M. Shi, and H. Ding, *Nat. Phys.* **11**, 724 (2015).
 - ¹² L.X. Yang, Z.K. Liu, Y. Sun, H. Peng, H.F. Yang, T. Zhang, B. Zhou, Y. Zhang, Y.F. Guo, M. Rahn, D. Prabhakaran, Z. Hussain, S.K. Mo, C. Felser, B. Yan, and Y.L. Chen, *Nat. Phys.* **11**, 728 (2015).
 - ¹³ S.Y. Xu, N. Alidoust, I. Belopolski, Z.J. Yuan, G. Bian, T.R. Chang, H. Zheng, V.N. Strocov, D.S. Sanchez, G.Q. Chang, C.L. Zhang, D.X. Mou, Y. Wu, L.N. Huang, C.C. Lee, S.M. Huang, B.K. Wang, A. Bansil, H.T. Jeng, T. Neupert, A. Kaminski, H. Lin, S. Jia, and M.Z. Hasan, *Nat. Phys.* **11**, 748 (2015).
 - ¹⁴ N. Xu, H.M. Weng, B.Q. Lv, C.E. Matt, J. Park, F. Bisti, V.N. Strocov, D. Gawryluk, E. Pomjakushina, K. Conder, N.C. Plumb, M. Radovic, G. Aútes, O.V. Yazyev, Z. Fang, X. Dai, T. Qian, J. Mesot, H. Ding, and M. Shi, *Nat. Commun.* **7**, 11006 (2016).
 - ¹⁵ A.A. Soluyanov, D. Gresch, Z.J. Wang, Q.S. Wu, M. Troyer, X. Dai, and B.A. Bernevig, *Nature* **527**, 495 (2015).
 - ¹⁶ M.O. Goerbig, J.-N. Fuchs, G. Montambaux, and F. Piéchon, *Phys. Rev. B* **78**, 045415 (2008).
 - ¹⁷ H.J. Noh, J. Jeong, E.J. Cho, K. Kim, B.I. Min, and B.G. Park, *Phys. Rev. Lett.* **119**, 016401 (2017).
 - ¹⁸ F.C. Fei, X.Y. Bo, R. Wang, B. Wu, J. Jiang, D.Z. Fu, M. Gao, H. Zheng, Y.L. Chen, X.F. Wang, H.J. Bu, F.Q. Song, X.G. Wang, B.G. Wang, and G.H. Wang, *Phys. Rev. B* **96**, 041201(R) (2017).
 - ¹⁹ M.Z. Yan, H.Q. Huang, K.N. Zhang, E. Wang, W. Yao, K. Deng, G.L. Wan, H.Y. Zhang, M. Arita, H.T. Yang, Z. Sun, H. Yao, Y. Wu, S.S. Fan, W.H. Duan, and S.Y. Zhou, *Nat. Commun.* **8**, 257 (2017).
 - ²⁰ M. Trescher, B. Sviderski, P.W. Brouwer, and E.J. Bergholtz, *Phys. Rev. B* **91**, 115135 (2015).
 - ²¹ I. Proskurin, M. Ogata, and Y. Suzumura, *Phys. Rev. B* **91**, 195413 (2015).
 - ²² T.E. O'Brien, M. Diez, and C.W.J. Beenakker, *Phys. Rev. Lett.* **116**, 236401 (2016).
 - ²³ Z.M. Yu, Y. Yao, and S.A. Yang, *Phys. Rev. Lett.* **117**, 077202 (2016).
 - ²⁴ M. Udagawa and E.J. Bergholtz, *Phys. Rev. Lett.* **117**, 086401 (2016).
 - ²⁵ S. Tchoumakov, M. Civelli, and M.O. Goerbig, *Phys. Rev. Lett.* **117**, 086402 (2016).
 - ²⁶ A.A. Zyuzin and R.P. Tiwari, *JETP Lett.* **103**, 717 (2016).
 - ²⁷ J.F. Steiner, A.V. Andreev, and D.A. Pesin, *Phys. Rev. Lett.* **119**, 036601 (2017).
 - ²⁸ Y. Ferreira, A.A. Zyuzin, and J.H. Bardarson, *Phys. Rev. B* **96**, 115202 (2017).
 - ²⁹ S. Saha and S. Tewari, arXiv:1707.04117.
 - ³⁰ J. González, F. Guinea, and M.A.H. Vozmediano, *Nucl. Phys. B* **424**, 595 (1994).
 - ³¹ J. González, F. Guinea, and M.A.H. Vozmediano, *Phys. Rev. B* **59**, R2474 (1999).
 - ³² D.T. Son, *Phys. Rev. B* **75**, 235423 (2007).
 - ³³ D.E. Sheehy and J. Schmalian, *Phys. Rev. Lett.* **99**, 226803 (2007).
 - ³⁴ H. Isobe and N. Nagaosa, *J. Phys. Soc. Jpn.* **81**, 113704 (2012).
 - ³⁵ H. Isobe and N. Nagaosa, *Phys. Rev. Lett.* **116**, 116803 (2016).
 - ³⁶ Z.M. Huang, J. Zhou and S.Q. Shen, *Phys. Rev. B* **95**, 195412 (2017).
 - ³⁷ R.R. Biswas, S. Sachdev, D.T. Son, *Phys. Rev. B* **76**, 205122 (2007).
 - ³⁸ G.Y. Cho and E.G. Moon, *Sci. Rep.* **6**, 19198 (2016).
 - ³⁹ F. Detassis, L. Fritz, and S. Grubinskas, arXiv: 1703.02425 (2017).
 - ⁴⁰ J. Polchinski, *Nucl. Phys. B* **422**, 617 (1994).
 - ⁴¹ C. Nayak and F. Wilczek, *Nucl. Phys. B* **430**, 534 (1994).
 - ⁴² M. Hermele, T. Senthil, M.P.A. Fisher, P.A. Lee, N. Nagaosa, and X.G. Wen, *Phys. Rev. B* **70**, 214437 (2004).
 - ⁴³ S.S. Lee, *Phys. Rev. B* **80**, 165102 (2009).
 - ⁴⁴ D.F. Mross, J. McGreevy, H. Liu, and T. Senthil, *Phys. Rev. B* **82**, 045121 (2010).